

Finite Sample Analysis of Open-loop Subspace Identification Methods

Jiabao He, Ingvar Ziemann, Cristian R. Rojas, S. Joe Qin and Håkan Hjalmarsson

Abstract—Subspace identification methods (SIMs) are known for their simple parameterization for MIMO systems and robust numerical properties. However, a comprehensive statistical analysis of SIMs remains an open problem. Following a three-step procedure generally used in SIMs, this work presents a finite sample analysis for open-loop SIMs. In Step 1 we begin with a parsimonious SIM. Leveraging a recent analysis of an individual ARX model, we obtain a union error bound for a Hankel-like matrix constructed from a bank of ARX models. Step 2 involves model reduction via weighted singular value decomposition (SVD), where we use robustness results for SVD to obtain error bounds on extended controllability and observability matrices, respectively. The final Step 3 focuses on deriving error bounds for system matrices, where two different realization algorithms, the MOESP type and the CVA type, are studied. Our results not only agree with classical asymptotic results, but also show how much data is needed to guarantee a desired error bound with high probability. The proposed method generalizes related finite sample analyses and applies broadly to many variants of SIMs.

Index Terms—subspace identification, finite sample analysis, state-space model, ARX model

I. INTRODUCTION

Originating from the celebrated Ho-Kalman algorithm [1], subspace identification methods (SIMs) have proven extremely useful for estimating linear state-space models and became one of the mainstream approaches in system identification. Over the past 50 years, numerous efforts have been made to develop improved algorithms and gain a deeper understanding of them. For a comprehensive overview of SIMs, we refer to [2], [3]. Overall speaking, SIMs can be categorized into two types, namely, the open-loop and closed-loop. Open-loop SIMs were developed first and formed the basis for the development of closed-loop ones. Some representative open-loop SIMs are canonical variate analysis (CVA) [4], numerical algorithms for subspace state-space system identification (N4SID) [5], multivariable output-error state-space (MOESP) algorithms

Jiabao He, Cristian R. Rojas and Håkan Hjalmarsson are with the Division of Decision and Control Systems, School of Electrical Engineering and Computer Science, KTH Royal Institute of Technology, 100 44 Stockholm, Sweden. (Emails: jiabao, crro, hjalmars@kth.se)

Ingvar Ziemann is with the University of Pennsylvania, Philadelphia, PA 19104 USA. (Email: ingvarz@seas.upenn.edu)

S. Joe Qin is with the Institute of Data Science, Lingnan University, Hong Kong (Email: joeqin@ln.edu.hk)

This work was supported by VINNOVA Competence Center Ad-BIOPRO, contract [2016-05181] and by the Swedish Research Council through the research environment NewLEADS (New Directions in Learning Dynamical Systems), contract [2016-06079], and contract 2019-04956.

[6], the observer-Kalman filter method (OKID) [7], and the parsimonious SIM (PARSIM) [8], [9]. Despite the significant theoretical and practical success of SIMs, certain limitations remain—most notably, their lower accuracy compared to the prediction error method (PEM) in the case of exogenous inputs being present, and the lack of a comprehensive statistical analysis. A thorough statistical analysis of SIMs is essential to establish their reliability, assess their performance, and guide the design of more robust and efficient algorithms and the choice of user choices.

A. Related Work

There are some significant contributions to statistical properties of SIMs in the asymptotic regime [10]–[23]. The consistency and asymptotic variance of SIMs are analyzed in [13], [21] and [16]–[20], respectively. In particular, it was pointed out in [13] that the persistence of excitation (PE) of inputs is not sufficient for consistency, and stronger conditions are required in some cases. In addition, the impact of some weighting matrices in the SVD step was discussed in [24], [25], which claim that the choices of weighting matrices mainly influence the asymptotic distribution of the estimates. Although the CVA method gives the lowest variance among available weighting choices when the measured inputs are white [11], there is no formal proof to show that it is asymptotically efficient [23]. In the asymptotic regime, convergence rates can be derived using the central limit theorem (CLT) or the law of the iterated logarithm (LIL) [26]. However, such results only hold as the number of samples tends to infinity. In reality, all data is finite. Asymptotic results serve primarily as heuristics and often fall short in capturing transient behaviors, explaining performance differences among SIM variants in finite sample settings, or determining how much data is needed to get a model with which we are satisfied.

There has been a recent resurgence of interest in identifying state-space models, where the focus is on the non-asymptotic regime. Finite sample analysis in the field of system identification was pioneered by [27], [28], where the performance of PEMs was analyzed. Over the last few years, a series of papers have revisited this topic and introduced many promising developments on fully observed systems [29]–[31] and partially observed systems [32]–[37]. For a broader overview of these results, we refer to [38]. As stated in [32], finite sample analysis has been a standard tool for comparing algorithms. Such an analysis of SIMs can provide a qualitative characterization of learning complexity and elucidate data-accuracy trade-offs. Moreover, it can guide the choice of user

choices, such as the horizons and weighting matrices, which may lead to an improvement of the estimator in a two-step approach. However, the path of finite sample analysis for SIMs proves to be challenging due to the involvement of multi-step statistical operations [19], such as regression, projection, weighted SVD and maximum likelihood (ML) estimation. While these steps enhance performance, they simultaneously pose challenges for any subsequent statistical analysis. Putting the studies on fully observed systems aside, the most relevant studies on partially observed systems are [32], [33], [36], [39]. However, they mainly analyze the performance of the Ho-Kalman algorithm or similar variants which are rarely used in practice, their results therefore are not sufficient to completely reveal statistical properties of SIMs actually deployed. To the best of our knowledge, a complete finite sample analysis of SIMs under general conditions is still an open problem.

B. Contributions

The main contributions of this paper are three-fold:

(1) We develop a robust and scalable framework for finite sample analysis of a broad class of SIMs. To avoid non-causal models caused by the projection step in classical SIMs, we propose to use PARSIM to enforce a causal model. Such a choice brings convenience to statistical analysis, and the method can be applied to other ARX-based SIMs, such as SSARX [40] and PBSID [21].

(2) We establish a more general PE condition. Compared with related studies that only include past inputs and past outputs as regressors, our work also includes future inputs as regressors, leading to a more general PE condition. This broader PE condition is instrumental in deriving error bounds and in analyzing the use of data-dependent weighting matrices. Therefore, it serves as a contribution of independent interest.

(3) Compared with related studies that streamline the realization algorithm, we provide the first finite sample upper bounds on system matrices under different weighting matrices and two popular realization algorithms.

A preliminary version [41] of this work was accepted by IEEE CDC24, where we provide a finite sample analysis for a simplified PARSIM, i.e., without taking into account the weighting matrices and including the CVA type realization algorithm. In this full version, we include different weighting matrices and two popular realization algorithms. In addition, we also provide complete proofs and a technical framework to approach this problem.

C. Structure

The disposition of the paper is as follows: In Section II, we introduce models and assumptions used in SIMs, and then formulate the problem explicitly. In Section III, we present a short review of SIMs with a focus on PARSIM, and the roadmap ahead to analyze its finite sample behavior. In Section IV, we first provide a finite sample analysis of an individual ARX model, which we then combine with a union bound to control the performance of a bank of ARX models. In Section V, we first analyze certain robustness properties of weighted SVD, and then derive error bounds on the system matrices coming from two realization algorithms.

In Section VI, we discuss the implications of our main results. Finally, the paper is concluded in Section VII. All proofs and technical lemmas are provided in the Appendix.

D. Notations

(1) For a matrix X with appropriate dimensions, X^\top , X^{-1} , $X^{\frac{1}{2}}$, X^\dagger , $\|X\|$, $\|X\|_F$, $\det(X)$, $\text{rank}(X)$, $\text{trace}(X)$, $\rho(X)$, $\lambda_{\max}(X)$, $\lambda_{\min}(X)$, $\sigma_{\min}(X)$ and $\sigma_n(X)$ denote its transpose, inverse, square root, Moore-Penrose pseudo-inverse, spectral norm, Frobenius norm, determinant, rank, trace, spectral radius, maximum eigenvalue, minimum eigenvalue, minimum singular value and n -th largest singular value, respectively. Moreover, $X_1 \succ (\succcurlyeq) 0$ and $X_2 \prec (\preccurlyeq) 0$ mean that X_1 is positive (semi) definite and X_2 is negative (semi) definite, respectively. $\text{diag}(X_1, X_2)$ is a block matrix having X_1 and X_2 on its diagonal. The matrices I and 0 are the identity and zero matrices with compatible dimensions.

(s) The multivariate normal distribution with mean μ and covariance Σ is denoted as $\mathcal{N}(\mu, \Sigma)$. The notation $\mathbb{E}[x]$ is the expectation of a random vector x . For an event \mathcal{E} , $\mathbb{P}(\mathcal{E})$ is the probability of \mathcal{E} , \mathcal{E}^c is the complementary event of \mathcal{E} , and $\mathcal{E}_1 \cup \mathcal{E}_2$ and $\mathcal{E}_1 \cap \mathcal{E}_2$ are the union and intersection of events \mathcal{E}_1 and \mathcal{E}_2 , respectively. We use $\mathbb{I}_{\{\mathcal{E}\}}$ to denote the indicator function of \mathcal{E} .

(3) The notation $f = \mathcal{O}(g)$ means that functions $f, g \in \mathbb{R}^d$ satisfy $\limsup_{x \rightarrow x_0} \left| \frac{f(x)}{g(x)} \right| < \infty$, where the limit point x_0 is typically understood from the context. Moreover, $f \gtrsim g$ means f is greater than or approximately equal to g .

(4) The notations c, c_1, \dots stand for universal constants independent of system parameters, confidence, and accuracy.

II. PROBLEM FORMULATION

A. Models and Assumptions

Consider the following discrete-time linear time-invariant (LTI) system in innovations form:

$$x_{k+1} = Ax_k + Bu_k + K\Sigma_e^{\frac{1}{2}}e_k, \quad (1a)$$

$$y_k = Cx_k + \Sigma_e^{\frac{1}{2}}e_k, \quad (1b)$$

where $x_k \in \mathbb{R}^{n_x}$, $u_k \in \mathbb{R}^{n_u}$, $y_k \in \mathbb{R}^{n_y}$ and $e_k \in \mathbb{R}^{n_y}$ are the state, input, output and innovations, respectively. For brevity of notation, we assume that the initial time starts at $k = 1$, and the terminal time is denoted as $\bar{N} = N + p + f - 1$, where N is the number of columns in data Hankel matrices, and p and f stand for past and future horizons, respectively, to be defined later. In addition, the initial state is assumed to be $x_1 = 0$. We make the following standard assumptions:

Assumption 2.1: (1) The spectral radius of A and A_K satisfy $\rho(A) < 1$ and $\rho(A_K) < 1$.

(2) The system is minimal, i.e., $(A, [B, K])$ is controllable and (A, C) is observable.

(3) The innovations $\{e_k\}$ consists of independent and identically distributed (i.i.d.) Gaussian random variables, i.e., $e_k \sim \mathcal{N}(0, I)$.¹

¹Similar to [42], our results can be extended to more general setups, such as sub-Gaussians.

(4) The input sequence $\{u_k\}$ consists also of i.i.d. Gaussian random variables, i.e., $u_k \sim \mathcal{N}(0, \sigma_u^2 I)$. Moreover, it is assumed independent of $\{e_k\}$.

Remark 1: To illustrate the generality of the innovations model (1), we consider the following standard state-space model which divides the noise term into contributions from measurement noise v_k acting on the outputs and process noise w_k acting on the states [43]:

$$x_{k+1} = Ax_k + Bu_k + w_k, \quad (2a)$$

$$y_k = Cx_k + v_k. \quad (2b)$$

The noises w_k and v_k consist of i.i.d. zero-mean Gaussian random variables, with covariance Σ_w and Σ_v , respectively. Moreover, they are independent of each other. We assume that $\Sigma_v \succ 0$, (A, C) is detectable, and (A, Σ_w) is stabilizable. Then, the Kalman filter of system (2) is well defined, and the Kalman gain is equal to

$$K = -APC^\top (CPC^\top + \Sigma_v)^{-1},$$

where P is the solution of the following Riccati equation:

$$P = APA^\top + \Sigma_w - APC^\top (CPC^\top + \Sigma_v)^{-1} (APC^\top)^\top.$$

We further assume that the initial state is a zero-mean Gaussian variable with covariance P and independent of the noises. Then, by the orthogonality principle the innovations sequence also consists of i.i.d. Gaussian variables with covariance

$$\Sigma_e = CPC^\top + \Sigma_v.$$

Therefore, under mild conditions the innovations form (1) describes the same input-output trajectories as the standard state-space model (2), and it is widely used in SIMs [2].

Based on the innovations form, after replacing $\Sigma_e^{1/2} e_k$ in (1a) with $y_k - Cx_k$, we obtain the following predictor form:

$$x_{k+1} = A_K x_k + Bu_k + Ky_k, \quad (3a)$$

$$y_k = Cx_k + \Sigma_e^{1/2} e_k, \quad (3b)$$

where $A_K = A - KC$. Since the innovations form and the predictor form are equivalent and all can represent input and output data exactly, one has the option to use any of these forms for convenience. For instance, MOESP [6] and PARSIM [8] use the innovations form, and SSARX [40] and PBSID [23] use the predictor form.

B. Problem Formulation

In this paper we tackle the following problem:

Problem 1: Given a finite number \bar{N} of input-output samples from a single trajectory of system (1), our goal is to explicitly derive high probability error bounds on the system matrices estimated by some SIMs. To be specific, given a confidence level $0 < \delta < 1$, we wish to derive error bounds $\epsilon_A, \epsilon_B, \epsilon_C$, such that

$$\|\hat{A} - T^{-1}AT\| \leq \epsilon_A, \quad \|\hat{B} - T^{-1}B\| \leq \epsilon_B, \quad \|\hat{C} - CT\| \leq \epsilon_C,$$

hold with probability at least $1 - \delta$, where \hat{A} , \hat{B} and \hat{C} are estimates of system matrices, and T is a non-singular matrix.

Remark 2: It is only possible to obtain the system matrices up to a similarity transformation due to the non-uniqueness of a realization [33]. Moreover, it should be mentioned that the matrix T here is stochastic, depending on the realization. Alternatively the estimates could be transformed into a canonical form. Furthermore, bounds on the estimation of Markov parameters or other system invariants could also be given.

Problem 1 is one of the long-standing open problems in subspace identification. As noted by Van Overschee and De Moor [44], “solving these problems would contribute significantly to the maturing of the field of subspace identification.” The existing literature already offers some pertinent solutions to Problem 1. According to recent work [32], [42] in the non-asymptotic regime, the error bound ϵ_θ is typically of the form

$$\epsilon_\theta \propto (\text{SNR})^{-1} \times \sqrt{\frac{\text{problem dimension} + \log(1/\delta)}{\bar{N}}}, \quad (4)$$

where θ denotes the parameter of interest, and SNR denotes the signal-to-noise ratio.

In the asymptotic regime, prior work [16]–[20] have shown that the normalized error $\sqrt{\bar{N}}(\hat{\theta} - \theta)$ converges in law to a normal distribution. Consequently, the results in (4)–where the error decays at rate $\mathcal{O}(1/\sqrt{\bar{N}})$ and the confidence level δ appears through $\log(1/\delta)$ –are consistent with these asymptotic results. Moreover, the LIL suggests that error decays at rate $\mathcal{O}(\sqrt{\frac{\log \log \bar{N}}{\bar{N}}})$ almost surely [10], which is sharp. However, asymptotic results require that $\bar{N} \rightarrow \infty$ and can only be used as a heuristic for a finite \bar{N} . Some questions remained unanswered. For instance, there often is a minimal requirement on \bar{N} , namely the burn-in time \bar{N}_{pe} , which is necessary for a bound of the form (4) to hold. Such requirements are typically of the form

$$\bar{N}_{\text{pe}} \gtrsim \text{problem dimension} + \log(1/\delta). \quad (5)$$

The above \bar{N}_{pe} cannot be obtained by applying only asymptotic tools [38]. Moreover, as shown in [32] and Lemma 1 in this work, non-asymptotic analysis can even achieve an error bound for marginally stable systems, whereas asymptotic results are often limited to asymptotically stable systems.

Existing non-asymptotic results for Problem 1 mainly focus on the classical Ho–Kalman algorithm or similar variants [32], [33], [35], [36]. However, this realization algorithm is outdated, as more powerful SIMs have later been proposed in the literature. Whether the structure in (4) also holds for modern SIMs has therefore remained unclear. This work proves that modern SIMs also obey the same structure. Moreover, it is different in the following key respects.

First, a standard step of SIMs is to estimate a Hankel (or Hankel-like) matrix of Markov parameters, denoted by \mathcal{H}_{fp} . A key feature of modern SIMs is that \mathcal{H}_{fp} is estimated directly using a projection method. However, this projection step couples future data with past data, resulting in an error without a standard martingale structure, which is difficult to upper bound. We believe that this is one of the main barriers preventing a finite sample analysis for SIMs. Previous analyses either revert to the Ho–Kalman algorithm [45] or avoid inputs [32], where the projection step is not involved,

thereby sidestepping the problem. The way we solve it is to absorb the projection matrix into an enlarged regressor, so that the error restores a standard martingale structure. The price to pay is that this format requires a more complex yet tractable PE condition.

Second, in the model reduction step, due to the fact that \mathcal{H}_{fp} is low-rank, some data-dependent weighting matrices W_1 and W_2 are pre-multiplied and post-multiplied to the estimate of \mathcal{H}_{fp} before performing an SVD to improve the numerical and statistical properties. Several asymptotic properties of such algorithmic variations have been studied in [19]. However, it is an open problem to study the impact of weighting matrices and compare their performance in a finite sample setting [38], [44]. Prior work [32], [35], [36], [45] considered the trivial weighting $W_1 = W_2 = I$. This work delivers the first finite sample analysis for general weighting matrices through a novel analysis leveraging the Schur complement.

Third, unlike the Ho-Kalman algorithm, many SIMs typically estimate system matrices by first recovering the state sequences and then applying least-squares regression in the output and state equations. To the best of our knowledge, this realization algorithm has not been analyzed in the non-asymptotic regime. Our work shows that the error of this realization algorithm also obeys the structure of (4).

In summary, our work extends finite sample results from simplified prototypes to the algorithms actually deployed, offering new insights and systematic performance guarantees.

III. A RECAP OF SUBSPACE IDENTIFICATION METHODS

In this section we provide a short overview of open-loop SIMs, with the focus on PARSIM. For convenience, we define

$$u_p(k) = [u_k^\top \ u_{k+1}^\top \ \cdots \ u_{k+p-1}^\top]^\top \in \mathbb{R}^{pn_u},$$

$$u_f(k) = [u_{k+p}^\top \ u_{k+p+1}^\top \ \cdots \ u_{k+p+f-1}^\top]^\top \in \mathbb{R}^{fn_u},$$

which stack past inputs and future inputs, respectively. Similar definitions apply to $y_p(k)$, $e_f(k)$, $u_i(k)$ and $e_i(k)$. Moreover, after lining up $u_p(k)$ and $u_f(k)$ from $k = 1$ to $k = N$, we obtain Hankel matrices

$$U_p = [u_p(1) \ u_p(2) \ \cdots \ u_p(N)], \quad (6a)$$

$$U_f = [u_f(1) \ u_f(2) \ \cdots \ u_f(N)]. \quad (6b)$$

Similar definitions apply to data matrices Y_p , Y_f , E_p and E_f [8]. The state sequence is given by

$$X_k = [x_k \ x_{k+1} \ \cdots \ x_{k+N-1}]. \quad (7)$$

By iterating model (1) using the above notations, an extended state-space model [8] can be derived as

$$Y_f = \Gamma_f X_k + G_f U_f + H_f E_f, \quad (8a)$$

$$Y_p = \Gamma_p X_{k-p} + G_p U_p + H_p E_p, \quad (8b)$$

where Γ_f is the extended observability matrix, defined by

$$\Gamma_f = [C^\top \ (CA)^\top \ \cdots \ (CA^{f-1})^\top]^\top. \quad (9)$$

Moreover, the transmission matrices G_f is a lower-triangular Toeplitz matrix of Markov parameters,

$$G_f = \begin{bmatrix} 0 & 0 & \cdots & 0 \\ CB & 0 & \cdots & 0 \\ \vdots & \vdots & \ddots & \vdots \\ CA^{f-2}B & CA^{f-3}B & \cdots & 0 \end{bmatrix}, \quad (10)$$

and H_f is similarly defined by replacing 0 on the diagonal of G_f with $\Sigma_e^{\frac{1}{2}}$, and by replacing B with $K\Sigma_e^{\frac{1}{2}}$. Similar definitions apply to matrices Γ_p , G_p and H_p . Furthermore, by iterating equation (3a), we obtain

$$X_k = L_p Z_p + A_K^p X_{k-p}, \quad (11)$$

where $Z_p = [Y_p^\top \ U_p^\top]^\top$ and L_p is the extended controllability matrix in a reverse order, defined by

$$L_p = [A_K^{p-1}K \ \cdots \ K \ A_K^{p-1}B \ \cdots \ B]. \quad (12)$$

After substituting (11) into (8a), we have

$$Y_f = \mathcal{H}_{fp} Z_p + G_f U_f + H_f E_f + \Gamma_f A_K^p X_{k-p}, \quad (13)$$

where $\mathcal{H}_{fp} := \Gamma_f L_p$ is the Hankel-like matrix. Most variants of SIMs can be integrated into a unified framework [2], [46] which generally consists of three steps. We now introduce them based on (13).

A. Step 1: Linear Regression or Projection

Most open-loop SIMs use (13) to first estimate the Hankel-like matrix \mathcal{H}_{fp} , and then proceed to obtain the system matrices. A basic approach in classical SIMs is one-step regression [5], [6], [13], [15], which takes Z_p and U_f as regressors and obtains \mathcal{H}_{fp} and G_f simultaneously using

$$\hat{\Theta} := [\hat{\mathcal{H}}_{fp} \ \hat{G}_f] = Y_f \begin{bmatrix} Z_p \\ U_f \end{bmatrix}^\dagger. \quad (14)$$

Since \mathcal{H}_{fp} is our main interest, using the inverse of a block matrix (see Lemma 16), $\hat{\mathcal{H}}_{fp}$ can be extracted from (14) as

$$\hat{\mathcal{H}}_{fp} = Y_f \Pi_{U_f}^\perp Z_p^\top (Z_p \Pi_{U_f}^\perp Z_p^\top)^{-1}, \quad (15)$$

where $\Pi_{U_f}^\perp = I - U_f^\top (U_f U_f^\top)^{-1} U_f$. Although the estimate $\hat{\mathcal{H}}_{fp}$ is consistent [15], the one-step regression method cannot preserve the lower-triangular Toeplitz structure of the transmission matrix G_f , which is responsible for recording the impact of future input U_f on future output Y_f . Due to the loss of this structure in \hat{G}_f , the model format is not causal anymore, which poses a challenge in statistical analysis.

Remark 3: In some literature of SIMs, the above one-step regression is called the projection method, in the sense that the future input U_f is first projected out using

$$Y_f \Pi_{U_f}^\perp = \Gamma_f L_p Z_p \Pi_{U_f}^\perp + H_f E_f \Pi_{U_f}^\perp + \Gamma_f A_K^p X_{k-p} \Pi_{U_f}^\perp. \quad (16)$$

For a sufficiently large p , since $A_K^p \approx 0$, the rightmost term $\Gamma_f A_K^p X_{k-p} \Pi_{U_f}^\perp$ becomes negligible. Moreover, as U_f is uncorrelated with E_f , we have $E_f \Pi_{U_f}^\perp \approx E_f$. After multiplying Z_p^\top on both sides of (16), we have

$$Y_f \Pi_{U_f}^\perp Z_p^\top \approx \Gamma_f L_p Z_p \Pi_{U_f}^\perp Z_p^\top + H_f E_f Z_p^\top. \quad (17)$$

Since E_f is uncorrelated with Z_p , implying $\frac{1}{N}E_fZ_p^\top \approx 0$, $\Gamma_f L_p$ can then be estimated using least-squares. It is clear that the estimate of $\Gamma_f L_p$ in (17) is identical to (15).

To enforce causal models, a parallel and parsimonious SIM, PARSIM, is proposed in [8]. Instead of using the one-step regression, PARSIM zooms into each row of (13) and performs f least-squares to estimate a bank of ARX models. To illustrate this, equation (13) can be partitioned row-wise as

$$Y_{fi} = \Gamma_{fi} L_p Z_p + G_{fi} U_i + H_{fi} E_i + \Gamma_{fi} A_K^p X_{k-p}, \quad (18)$$

where for $i = 1, 2, \dots, f$, $\Gamma_{fi} = CA^{i-1} \in \mathbb{R}^{n_y \times n_x}$,

$$\begin{aligned} Y_{fi} &= [y_{k+i-1} \ y_{k+i} \ \cdots \ y_{k+N+i-2}] \in \mathbb{R}^{n_y \times N}, \\ U_{fi} &= [u_{k+i-1} \ u_{k+i} \ \cdots \ u_{k+N+i-2}] \in \mathbb{R}^{n_u \times N}, \\ U_i &= [U_{f1}^\top \ U_{f2}^\top \ \cdots \ U_{fi}^\top]^\top \in \mathbb{R}^{in_u \times N}, \\ G_{fi} &= [CA^{i-2}B \ \cdots \ CB \ 0] \in \mathbb{R}^{n_y \times in_u}, \\ H_{fi} &= [CA^{i-2}K\Sigma_e^{\frac{1}{2}} \ \cdots \ CK\Sigma_e^{\frac{1}{2}} \ \Sigma_e^{\frac{1}{2}}] \in \mathbb{R}^{n_y \times in_y}, \end{aligned}$$

where similar definitions apply to E_{fi} and E_i . PARSIM then minimizes a bank of i -steps ahead prediction errors from model (18) using ordinary least-squares (OLS),

$$\hat{\Theta}_i := \left[\widehat{\Gamma_{f1} L_p} \ \hat{G}_{fi} \right] = Y_{fi} \begin{bmatrix} Z_p \\ U_i \end{bmatrix}^\dagger. \quad (19)$$

At last, the whole estimate of \mathcal{H}_{fp} is obtained by stacking the f estimates together as

$$\hat{\mathcal{H}}_{fp} = \left[\widehat{\Gamma_{f1} L_p}^\top \ \widehat{\Gamma_{f2} L_p}^\top \ \cdots \ \widehat{\Gamma_{ff} L_p}^\top \right]^\top. \quad (20)$$

It has been shown in [8] that the estimate in (20) admits a smaller variance than (15).

B. Step 2: Weighted SVD

Since \mathcal{H}_{fp} has rank equal to n_x , to recover the extended observability matrix Γ_f and controllability matrix L_p from the estimate of \mathcal{H}_{fp} , weighted SVD is often used, i.e.,

$$W_1 \hat{\mathcal{H}}_{fp} W_2 = \hat{U} \hat{\Lambda} \hat{V}^\top \approx \hat{U}_1 \hat{\Lambda}_1 \hat{V}_1^\top, \quad (21)$$

where $\hat{\Lambda}_1$ contains the n_x largest singular values. In this way, a balanced realization of $\hat{\Gamma}_f$ and \hat{L}_p is

$$\hat{\Gamma}_f = W_1^{-1} \hat{U}_1 \hat{\Lambda}_1^{\frac{1}{2}}, \hat{L}_p = \hat{\Lambda}_1^{\frac{1}{2}} \hat{V}_1^\top W_2^{-1}. \quad (22)$$

Different choices of weighting matrices W_1 and W_2 lead to different variants of SIMs [2], [46]. Popular candidates of weighting matrices are summarized in Table I.²

C. Step 3: Realization of System Matrices

Given estimates of Γ_f and L_p , there are two paths to obtain the system matrices. It should be mentioned that currently there is no solid conclusion on which realization leads to a better model. To be specific, one is the CVA type which

²Notice that those weightings are normalized and may not be the same as they appear in the referred papers. These weightings, however, give estimates of Γ_f and L_p identical to those obtained using the original choice of weighting [13].

TABLE I
CANDIDATES OF WEIGHTING MATRICES

Method	W_1	W_2
OKID [7]	I	I
N4SID [5]	I	$(\frac{1}{N}Z_p Z_p^\top)^{\frac{1}{2}}$
MOESP [47]	I	$(\frac{1}{N}Z_p \Pi_{U_f}^\perp Z_p^\top)^{\frac{1}{2}}$
IVM [48]	$(\frac{1}{N}Y_f \Pi_{U_f}^\perp Y_f^\top)^{-\frac{1}{2}}$	$(\frac{1}{N}Z_p \Pi_{U_f}^\perp Z_p^\top)(\frac{1}{N}Z_p Z_p^\top)^{-\frac{1}{2}}$
CVA [4]	$(\frac{1}{N}Y_f \Pi_{U_f}^\perp Y_f^\top)^{-\frac{1}{2}}$	$(\frac{1}{N}Z_p \Pi_{U_f}^\perp Z_p^\top)^{\frac{1}{2}}$

uses the following linear regressions in the output and state equations to estimate the system matrices:

$$Y_{f1} = CX_k + \Sigma_e^{\frac{1}{2}} E_{f1}, \quad (23a)$$

$$X_k^+ = AX_k + BU_{f1} + K\Sigma_e^{\frac{1}{2}} E_{f1}, \quad (23b)$$

where X_k^+ stacks the states for the next time instant compared to X_k . By replacing X_k and X_k^+ with their estimates

$$\hat{X}_k = \hat{L}_p Z_p, \hat{X}_k^+ = \hat{L}_p Z_p^+, \quad (24)$$

where Z_p^+ is similarly defined as X_k^+ , we have

$$\hat{C} = Y_{f1} \hat{X}_k^\dagger, \quad (25a)$$

$$[\hat{A} \ \hat{B}] = \hat{X}_k^+ \begin{bmatrix} \hat{X}_k \\ U_{f1} \end{bmatrix}^\dagger. \quad (25b)$$

Another realization method is the MOESP type, which directly extracts system matrices based on the shift invariance property of $\hat{\Gamma}_f$ and \hat{L}_p , i.e.,

$$\hat{C} = \hat{\Gamma}_f(1 : n_y, :), \quad (26a)$$

$$\hat{A} = (\hat{\Gamma}_f^-)^\dagger \hat{\Gamma}_f^+, \quad (26b)$$

$$\hat{B} = \hat{L}_p(:, (2p-1)n_y + 1 : 2pn_y), \quad (26c)$$

where $\hat{\Gamma}_f^+$ and $\hat{\Gamma}_f^-$ are the last and first $f-1$ row blocks of $\hat{\Gamma}_f$, and the indexing of matrices follows MATLAB syntax.

Remark 4: In this paper, our main interest is to estimate the system matrices $\{A, B, C\}$, and derive error bounds for them. In principle, the Kalman gain K can also be obtained from the above algorithms with minor modifications. Meanwhile, there are also other methods to obtain K , such as solving a Riccati equation in N4SID and using QR factorization in PARSIM. To keep our results relatively compact, the estimate of K and its error bound are not considered in this work.

D. Roadmap Ahead

Now we sketch the path ahead to the solution for Problem 1. In the first step that estimates the Hankel-like matrix \mathcal{H}_{fp} , we opt for PARSIM to facilitate the analysis. Parallel to the three steps in SIMs, we solve Problem 1 by a three-step procedure:

(1) Step 1: We first derive an error bound on $\hat{\Theta}_i$ in (19) for every ARX model (18). In other words, we define the following events for $i = 1, 2, \dots, f$:

$$\mathcal{E}_{i,\Theta} := \left\{ \left\| \hat{\Theta}_i - \Theta_i \right\| \leq \epsilon_{\Theta_i} \right\}, \quad (27)$$

and require that $\mathbb{P}(\mathcal{E}_{i,\Theta}^c) \leq \frac{\delta}{f}$. We then utilize a norm inequality (see Lemma 15) between the block matrix $\widehat{\Gamma_f L_p} - \Gamma_f L_p$

and its sub-blocks $\widehat{\Gamma_{fi}L_p} - \Gamma_{fi}L_p$ to obtain the total bound on $\widehat{\mathcal{H}}_{fp} - \mathcal{H}_{fp}$. This essentially requires that the intersection of f events has probability $\mathbb{P}(\bigcap_{i=1}^f \mathcal{E}_{i,\Theta}) \geq 1 - \delta$, which is guaranteed due to the union bound $\mathbb{P}(\bigcup_{i=1}^f \mathcal{E}_{i,\Theta}^c) \leq \delta$.

(2) Step 2: We use recent results from SVD robustness [33], [49] to provide error bounds on the extended observability matrix Γ_f and controllability matrix L_p , where the impact of different weighting matrices in Table I is also discussed.

(3) Step 3: We derive error bounds ϵ_A , ϵ_B , and ϵ_C on the system matrices $\{A, B, C\}$ coming from the Larimore and MOESP realization algorithms.

IV. FINITE SAMPLE ANALYSIS OF ARX MODELS

Following our roadmap, we formalize Step 1 above in this section. We emphasize that the results presented in this section apply to each ARX model in (18) for $i = 1, \dots, f$, where the subscript i shows the model-specific dependence. For convenience, we define two covariates

$$\phi_{p,i}(k) = [y_p^\top(k) \ u_p^\top(k) \ u_i^\top(k)]^\top \in \mathbb{R}^{d_{p,i}}, \quad (28a)$$

$$w_{p,i}(k) = \Lambda_{u,e}^{-1} [u_p^\top(k) \ u_i^\top(k) \ e_p^\top(k)]^\top \in \mathbb{R}^{d_{p,i}}, \quad (28b)$$

where $d_{p,i} = p(n_u + n_y) + in_u$ is the problem dimension of each ARX model, and $\Lambda_{e,u} = \text{diag}(\sigma_u, \dots, \sigma_u, 1, \dots, 1)$ normalizes $w_{p,i}(k)$, such that it has unite variance. We further partition the following matrices column-wise:

$$\Phi_{p,i} = [\phi_{p,i}(1) \ \phi_{p,i}(2) \ \dots \ \phi_{p,i}(N)], \quad (29a)$$

$$E_i = [e_i(1) \ e_i(2) \ \dots \ e_i(N)], \quad (29b)$$

$$W_{p,i} = [w_{p,i}(1) \ w_{p,i}(2) \ \dots \ w_{p,i}(N)]. \quad (29c)$$

Moreover, we have the following definitions regarding the covariance and empirical covariance of $\phi_{p,i}(k)$ and x_k :

$$\Sigma_{p,i,k} := \mathbb{E} [\phi_{p,i}(k)\phi_{p,i}^\top(k)], \quad (30a)$$

$$\hat{\Sigma}_{p,i,N} := \frac{1}{N} \sum_{k=1}^N \phi_{p,i}(k)\phi_{p,i}^\top(k), \quad (30b)$$

$$\Sigma_{x,k} := \mathbb{E} [x_k x_k^\top]. \quad (30c)$$

Note that the regressor in (19) can be rewritten as

$$\Phi_{p,i} := \begin{bmatrix} Z_p \\ U_i \end{bmatrix} = \begin{bmatrix} Y_p \\ U_p \\ U_i \\ U_i \end{bmatrix} = \mathcal{O}_{p,i} X_{k-p} + \mathcal{T}_{p,i} \Lambda_{u,e} W_{p,i}, \quad (31)$$

where

$$\mathcal{O}_{p,i} = \begin{bmatrix} \Gamma_p \\ 0 \\ 0 \end{bmatrix}, \quad W_{p,i} = \Lambda_{u,e}^{-1} \begin{bmatrix} U_p \\ U_i \\ E_p \end{bmatrix}, \quad \mathcal{T}_{p,i} = \begin{bmatrix} G_p & 0 & H_p \\ I & 0 & 0 \\ 0 & I & 0 \end{bmatrix}.$$

Then, the error of the OLS estimate (19) can be written as

$$\begin{aligned} \tilde{\Theta}_i := \hat{\Theta}_i - \Theta_i &= H_{fi} E_i \Phi_{p,i}^\dagger + \Gamma_{fi} A_K^p X_{k-p} \Phi_{p,i}^\dagger \\ &= H_{fi} \underbrace{\sum_{k=1}^N \frac{1}{N} e_i(k) \phi_{p,i}^\top(k) \left(\hat{\Sigma}_{p,i,N}^{-1} \right)}_{\text{cross-term error } \tilde{\Theta}_i^E} + \\ &\quad \underbrace{\Gamma_{fi} A_K^p \sum_{k=1}^N \frac{1}{N} x_k \phi_{p,i}^\top(k) \left(\hat{\Sigma}_{p,i,N}^{-1} \right)}_{\text{truncation bias } \tilde{\Theta}_i^B}. \end{aligned} \quad (32)$$

There are two types of errors, namely, the cross-term error $\tilde{\Theta}_i^E$ and the truncation bias $\tilde{\Theta}_i^B$. A key observation is that the future innovations $e_i(k)$ are independent of the covariate $\phi_{p,i}(l)$ for all $l < k$. This provides a martingale structure, which is convenient to analyze. To bound the above two errors, we first use results from the smallest eigenvalue of the empirical covariance of causal Gaussian processes to lower bound $\hat{\Sigma}_{p,i,N}$ [36], [42], [50], which simultaneously establish the PE condition.

A. Persistence of Excitation

To achieve PE, the number of samples N should exceed a certain threshold, which we call the burn-in time N_{pe} .

Definition 4.1: Given a failure probability $0 < \delta < 1$, a past horizon p , and a future horizon i in each ARX model, the burn-in time N_{pe} is defined as

$$N_{pe}(\delta, p, i) = \min \{N : N \geq N_W(\delta, p, i), N_\Phi(\delta, p, i)\}, \quad (33)$$

where $N_W(\delta, p, i)$ and $N_\Phi(\delta, p, i)$ are defined in (I.11) and (I.18), respectively.

Remark 5: As shown in Appendix I, for any given p , i and δ , the N -dependent factors $N_W(\delta, p, i)$ and $N_\Phi(\delta, p, i)$ grow at most logarithmically with N . Therefore, for a sufficiently large N , the existence of $N_{pe}(\delta, p, i)$ is guaranteed.

A condition on PE is given by the following lemma:

Lemma 1: Fix a failure probability $0 < \delta < 1$. If $N \geq N_{pe}(\frac{\delta}{3}, p, i)$, then, we have that with probability at least $1 - \delta$,

$$\hat{\Sigma}_{p,i,N} \succcurlyeq \bar{\sigma}_{p,i}^2 I, \quad (34)$$

where $\bar{\sigma}_{p,i} := \frac{\|\mathcal{T}_{p,i}\| \|\Lambda_{u,e}\|}{2} > 0$.

Proof: See Appendix I. \blacksquare

Remark 6: Some relevant PE conditions appear in [32] and [36], where past outputs and inputs are included in regressors. Our analysis extends this by additionally incorporating future inputs, thus establishing a more general PE condition. This broader result is also useful for analyzing data-dependent weighting matrices, as detailed in Section V. Furthermore, this PE condition also holds for marginally stable systems.

B. Bound on Cross-term Error

Based on Lemma 1, an upper bound on the cross-term error $\tilde{\Theta}_i^E$ in (32) is provided in the following lemma:

Lemma 2: Fix a failure probability $0 < \delta < 1$. If $N \geq N_{pe}(\frac{\delta}{9}, p, i)$, then with probability at least $1 - \delta$, we have

$$\|\tilde{\Theta}_i^E\|^2 \leq c_1 \frac{\epsilon_{i,E}^2}{N}, \quad (35)$$

where $\epsilon_{i,E}^2 = \frac{\|H_{fi}\|^2}{\bar{\sigma}_{p,i}^2} \left(d_{p,i} \log \frac{d_{p,i}}{\delta} + \log \left(\det \left(\frac{\hat{\Sigma}_{p,i,N}}{\bar{\sigma}_{p,i}^2} \right) \right) \right)$.

Proof: See Appendix II. \blacksquare

C. Bound on Truncation Bias

In order to ensure that the truncation bias term $\tilde{\Theta}_i^B$ decays much faster than the cross-term error $\tilde{\Theta}_i^E$, we make the following assumption regarding the past horizon p .

Assumption 4.1: The past horizon is chosen as $p = \beta \log N$, where β is large enough such that

$$\|CA_K^p\| \|\Sigma_{x,N}\| \leq N^{-3}. \quad (36)$$

Remark 7: To ensure that the model (18) closely approximates an ARX model, the truncation bias $\Gamma_{fi} A_K^p x_k$ should be small enough, which requires that the exponentially decaying term A_K^p counteracts the magnitude of the state x_k . To illustrate this, we have that

$$\|\Sigma_{x,N}\| \leq \left\| \begin{bmatrix} B & K \end{bmatrix} \begin{bmatrix} \sigma_e^2 I & 0 \\ 0 & \Sigma_e \end{bmatrix} \begin{bmatrix} B^\top \\ K^\top \end{bmatrix} \right\| \sum_{k=0}^{N-1} \|A^k\|^2.$$

As a consequence of Lemma 19, the state norm $\|\Sigma_{x,N}\|$ grows at most polynomially with N . Meanwhile, since $\rho(A_K) < 1$, we have $\|A_K^p\| = \mathcal{O}(\bar{\rho}^p)$ for some $\bar{\rho} > \rho(A_K)$. Taking $p = \beta \log N$, we have $\|A_K^p\| = \mathcal{O}(N^{-\beta/\log(1/\bar{\rho})})$, which implies that the condition (36) is guaranteed for a large enough β .

Under Assumption 4.1, a bound on the bias term $\tilde{\Theta}_i^B$ in (32) is provided in the following lemma:

Lemma 3: Fix a failure probability $0 < \delta < 1$. If $N \geq N_{pe}(\frac{\delta}{9}, \beta \log N, i)$, then with probability at least $1 - \delta$, we have

$$\|\tilde{\Theta}_i^B\|^2 \leq c_2 \frac{\epsilon_{i,B}^2}{N^2}, \quad (37)$$

where $\epsilon_{i,B}^2 = \frac{n_x}{\sigma_{p,i}^2} \log \frac{1}{\delta}$.

Proof: See Appendix III. \blacksquare

D. Overall Bound

Lemma 2 suggests that the cross-term error $\tilde{\Theta}_i^E$ decays as $\mathcal{O}(1/\sqrt{N})$, and Lemma 3 suggests that the truncation bias $\tilde{\Theta}_i^B$ decays as $\mathcal{O}(1/N)$. This implies that $\tilde{\Theta}_i^B$ is dominated by $\tilde{\Theta}_i^E$ and it can be considered negligible. After absorbing higher order terms into the dominant term by inflating the constants accordingly, we obtain the following theorem controlling the whole error $\tilde{\Theta}_i$ of each ARX model in our collection.

Theorem 4.1: Fix a failure probability $0 < \delta < 1$. If $N \geq N_{pe}(\frac{\delta}{9}, \beta \log N, i)$, then with probability at least $1 - 2\delta$, we have

$$\|\tilde{\Theta}_i\|^2 \leq c \frac{\epsilon_{i,E}^2}{N}. \quad (38)$$

After obtaining an error bound on $\tilde{\Theta}_i$ in each ARX model, we proceed to bound the total error of \mathcal{H}_{fp} , which is crucial for our subsequent analysis. Based on the norm relation between a block matrix and its blocks in Lemma 15, it is straightforward to obtain a total bound on $\hat{\mathcal{H}}_{fp} - \mathcal{H}_{fp}$ from each bound $\|\tilde{\Theta}_i\|$.

Theorem 4.2: Fix a failure probability $0 < \delta < 1$. If $N \geq \max_{1 \leq i \leq f} \{N_{pe}(\frac{\delta}{9f}, \beta \log N, i)\}$, then with probability at least $1 - 2\delta$, we have

$$\|\hat{\mathcal{H}}_{fp} - \mathcal{H}_{fp}\| \leq \sqrt{f} \max_{1 \leq i \leq f} \|\tilde{\Theta}_i\| \leq \sqrt{\frac{cf}{N}} \max_{1 \leq i \leq f} \epsilon_i, \quad (39)$$

where $\epsilon_i^2 = \frac{\|H_{fi}\|^2}{\sigma_{p,i}^2} \left(d_{p,i} \log \frac{d_{p,i}f}{\delta} + \log \left(\det \left(\frac{\Sigma_{p,i,N}}{\sigma_{p,i}^2} \right) \right) \right)$.

V. ROBUSTNESS OF BALANCED REALIZATION

Following our roadmap, having obtained an overall error bound on $\hat{\mathcal{H}}_{fp} - \mathcal{H}_{fp}$ in Step 1, we now move to Step 2 to derive error bounds on the extended controllability and observability matrices, and Step 3 to obtain error bounds on the system matrices.

A. Weighted Singular Value Decomposition

Weighted SVD is crucial for improving the performance of SIMs. As summarized in Table I, different choices of weighting matrices lead to different variants of SIMs. Since those data-dependent weighting matrices share a similar structure, we choose the pair used in MOESP and PARSIM to illustrate their characteristics, where

$$W_1 = I, W_2 = \left(\frac{1}{N} Z_p \Pi_{U_f}^\perp Z_p^\top \right)^{\frac{1}{2}}. \quad (40)$$

The focus is on the data-dependent W_2 , whose finite-sample properties are summarized as follows:³

Lemma 4: Fix a failure probability $0 < \delta < 1$. If $N \geq N_{pe}(\delta, p, f)$, then with probability at least $1 - 3\delta/2 - \delta_u$, where $\delta_u = (2(N+f-1)n_u)^{-\log^2(2fn_u)\log(2(N+f-1)n_u)}$, the weighting matrix W_2 in (40) satisfies:

- (1) W_2 is positive definite.
- (2) $\|W_2\|$ grows at most logarithmically with N .
- (3) $\|W_2^{-1}\|$ is bounded.

Proof: See Appendix IV. \blacksquare

Now we study the robustness of SVD. Since other weighting matrices in Table I have the same properties as in Lemma 4, we will henceforth not specify a pair but use W_1 and W_2 to represent them universally. For simplicity, we further assume that W_1 and W_2 satisfy the conditions in Lemma 4 almost surely. The weighted SVD of the true value of \mathcal{H}_{fp} is

$$W_1 \mathcal{H}_{fp} W_2 = [U_1 \ U_0] \begin{bmatrix} \Lambda_1 & 0 \\ 0 & 0 \end{bmatrix} [V_1 \ V_0]^\top, \quad (41)$$

where $\Lambda_1 \succ 0$ contains the n_x largest singular values. A balanced realization for Γ_f and L_p is

$$\bar{\Gamma}_f = W_1^{-1} U_1 \Lambda_1^{1/2}, \bar{L}_p = \Lambda_1^{1/2} V_1^\top W_2^{-1}. \quad (42)$$

Then, we obtain the following robustness results regarding the estimates of Γ_f and L_p .

Theorem 5.1: If the following condition is satisfied:

$$\|W_1 \hat{\mathcal{H}}_{fp} W_2 - W_1 \mathcal{H}_{fp} W_2\| \leq \frac{\sigma_{n_x}(W_1 \mathcal{H}_{fp} W_2)}{4}, \quad (43)$$

then there exists an orthogonal matrix T , such that for a failure probability $0 < \delta < 1$, if $N \geq \max_{1 \leq i \leq f} \{N_{pe}(\frac{\delta}{9f}, \beta \log N, i)\}$, then with probability at least $1 - 2\delta$, we have

$$\|\hat{\Gamma}_f - \bar{\Gamma}_f T\| \leq \sqrt{\frac{40n_x}{\sigma_{n_x}(\mathcal{H}_{fp})}} \|\hat{\mathcal{H}}_{fp} - \mathcal{H}_{fp}\| W_\Gamma, \quad (44a)$$

$$\|\hat{L}_p - T^\top \bar{L}_p\| \leq \sqrt{\frac{40n_x}{\sigma_{n_x}(\mathcal{H}_{fp})}} \|\hat{\mathcal{H}}_{fp} - \mathcal{H}_{fp}\| W_L, \quad (44b)$$

where $W_\Gamma = \|W_1\| \|W_2\| \|W_1^{-1}\|^{\frac{3}{2}} \|W_2^{-1}\|^{\frac{1}{2}}$ and $W_L = \|W_1\| \|W_2\| \|W_2^{-1}\|^{\frac{3}{2}} \|W_1^{-1}\|^{\frac{1}{2}}$.

Proof: See Appendix IV. \blacksquare

Remark 8: Compared to a stochastic non-singular matrix T in Problem 1, matrix T is constrained to be an orthogonal matrix in Theorem 5.1. This is mainly due to Lemma 17.

³Similarly, conditions for other weighting matrices in Table I can be obtained.

Furthermore, according to the eigenvalue decomposition, every non-singular matrix has an associated orthogonal matrix. Therefore, such a constraint will not affect the generality of our results.

B. Bounds on System Matrices

Having obtained upper bounds on the extended observability matrix $\bar{\Gamma}_f$ and controllability matrix \bar{L}_p in Step 2, we now move to the final Step 3 to derive error bounds on the system matrices, where two realization algorithms are studied.

1) *CVA Type Realization*: The error bounds on system matrices from the realization algorithm (25) are follows:

Theorem 5.2: If the condition (43) is satisfied, then there exists an orthogonal matrix T , such that for a failure probability $0 < \delta < 1$, if $N \geq \max_{1 \leq i \leq f} \{N_{pe}(\delta/(9f), \beta \log N, i)\}$, then with probability at least $1 - 2\delta$, we have

$$\|\hat{C} - \bar{C}T\| \leq c_4 \|\hat{L}_p - T^\top \bar{L}_p\| + c_5 \frac{\epsilon_{0,B}}{N} + c_6 \frac{\epsilon_{0,E}}{\sqrt{N}}, \quad (45a)$$

$$\begin{aligned} \max \left\{ \|\hat{A} - T^\top \bar{A}T\|, \|\hat{B} - T^\top \bar{B}\| \right\} \leq \\ c_7 \|\hat{L}_p - T^\top \bar{L}_p\| + c_8 \frac{\epsilon_{1,B}}{N} + c_9 \frac{\epsilon_{1,E}}{\sqrt{N}}, \end{aligned} \quad (45b)$$

where detailed expressions of $c_4, \dots, c_9, \epsilon_{0,B}, \epsilon_{0,E}, \epsilon_{1,B}$ and $\epsilon_{1,E}$ are given in Appendix V.

Proof: See Appendix V. \blacksquare

2) *MOESP Type Realization*: The error bounds on system matrices from the realization algorithm (26) are follows:

Theorem 5.3: If the condition (43) is satisfied, then there exists an orthogonal matrix T , such that for a failure probability $0 < \delta < 1$, if $N \geq \max_{1 \leq i \leq f} \{N_{pe}(\delta/(9f), \beta \log N, i)\}$, then with probability at least $1 - 2\delta$, we have

$$\|\hat{C} - \bar{C}T\| \leq \|\hat{\Gamma}_f - \bar{\Gamma}_f T\|, \quad (46a)$$

$$\|\hat{B} - T^\top \bar{B}\| \leq \|\hat{L}_p - T^\top \bar{L}_p\|, \quad (46b)$$

$$\|\hat{A} - T^\top \bar{A}T\| \leq \frac{\sqrt{\|\Gamma_f L_p\|} + \sigma_o}{\sigma_o} \|\hat{\Gamma}_f - \bar{\Gamma}_f T\|, \quad (46c)$$

where $\sigma_o = \min \left(\sigma_{n_x}(\hat{\Gamma}_f^-), \sigma_{n_x}(\bar{\Gamma}_f^-) \right)$.

Proof: See Appendix V. \blacksquare

VI. DISCUSSIONS

We now discuss the implications of our main results. Specifically, we will answer two key questions: how to extend our method to other variants of SIMs, and what does the finite sample analysis bring.

A. Extensions to Other Methods

It is clear that our results in Steps 2 and 3 cover a large class of SIMs. In Step 1, to strictly enforce a causal model, we opt for the multi-regression method used in PARSIM—one of the most appealing SIMs, to estimate the Hankel-like matrix \mathcal{H}_{fp} . The following observations suggest that the technique used in the analysis of PARSIM can be extended to other SIMs.

First, our analysis for PARSIM can be extended to the one-step regression method in (15). If we study the estimation error of \mathcal{H}_{fp} in (15) separately, the cross-term error will

be $E_f \Pi_{U_f}^\perp Z_p^\top (Z_p \Pi_{U_f}^\perp Z_p^\top)^{-1}$. Due to the data-dependent projection matrix $\Pi_{U_f}^\perp$, the columns of E_f and Z_p are mixed together, bringing challenges to statistical analysis. However, this problem can be avoided if we study the total error of Θ in (14), which is equivalent to setting $i = f$ in PARSIM.

Second, our analysis can be extended to other SIMs that estimate high order ARX models using least-squares in their first step, such as SSARX [40] and PBSID [21]. To be specific, for SSARX, it first estimates the predictor Markov parameters $\{CA_K^i B, CA_K^i K\}_{i=0}^{f-1}$ from a high-order ARX model, and then replaces the true Markov parameters in the transmission matrices with their estimates, and proceeds to estimate a Hankel-like matrix. PBSID, also known as the whitening filter approach [21], starts from the predictor form (3). Similar to PARSIM, it utilizes the structure of the transmission matrices to carry out multiple regressions parallelly. It is clear that our methods can be applied to the first step of SSARX, and to every step of PBSID in the open-loop setting.

B. What Does Finite Sample Analysis Bring

Under the umbrella of this question, we analyze the implications of our results and validate them with simulations on a benchmark SISO system used in SIM studies [23]. It should be mentioned that the results in this paper directly extend to MIMO systems. The SISO system is given by

$$y_k + ay_{k-1} = bu_{k-1} + e_k + ce_{k-1}, \quad (47)$$

where $a = -0.7$, $b = 1$ and $c = 0.5$. The innovations $e_k \sim \mathcal{N}(0, 4)$. Two types of inputs are considered, one is a white input given by $u_k \sim \mathcal{N}(0, 1)$, and the other is a colored input⁴, generated by a white noise $r_k \sim \mathcal{N}(0, 1)$ passing through a filter $H_u(q^{-1}) = \frac{0.318}{1 - 0.5q^{-1} + 0.9q^{-2}}$, where q^{-1} is the backward shift operator.

1) *Statistical Rates*: According to Theorems 4.2, 5.1, 5.2 and 5.3, the error bounds on the Hankel-like matrix \mathcal{H}_{fp} , the extended observability matrix $\bar{\Gamma}_f$, controllability matrix \bar{L}_p , and system matrices C, B and A decay as $\mathcal{O}(1/\sqrt{N})$ up to logarithmic terms. Classical asymptotic results, such as the LIL, can tighten the log factor to $\mathcal{O}(\log \log N / \sqrt{N})$ [10]. This suggests that our bounds are not tight, which is one of the downsides of the non-asymptotic analysis. It is possible to optimize our results in the future.

2) *Persistence of Excitation*: Similar to the PE condition for consistency analysis in the asymptotic regime [13], Lemma 1 provides a non-asymptotic PE condition. Specifically, it guarantees the invertibility of the empirical covariance matrix $\hat{\Sigma}_{p,i,N}$ defined in (30) by establishing a lower bound on its smallest eigenvalue. In practice, once data is available, one can directly verify PE by computing the smallest eigenvalue of $\hat{\Sigma}_{p,i,N}$. Nonetheless, Lemma 1 provides a theoretical threshold, denoted by the burn-in time N_{pe} in (33), indicating the minimum sample size required to ensure invertibility of $\hat{\Sigma}_{p,i,N}$. Such a non-asymptotic result is valuable for designing experiments (e.g., determining excitation duration), and implementing stopping rules in adaptive control [31].

⁴It is important to note that due to Assumption 2.1, our theoretical results do not apply to scenarios with colored inputs yet. However, using colored inputs in our simulations helps in demonstrating the behavior of SIMs.

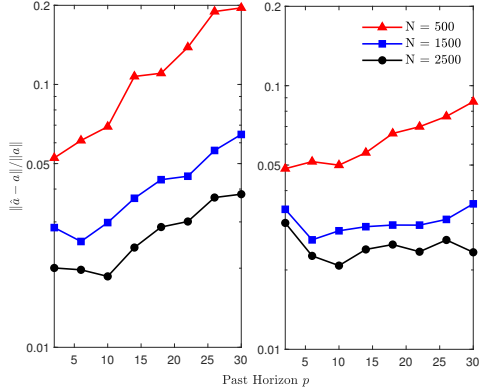


Fig. 1. A sweet spot for past horizon: MOESP (left) and CVA (right) realizations.

3) *Dimensional Dependence*: As shown in (33) and Theorem 4.2, the burn-in time N_{pe} and error bounds scale with the problem dimension $d_{p,i}$ and the state dimension n_x . Such a dimensional dependence still holds when n_x increases to the same order as N , whereas the results in the asymptotic regime are less meaningful in this case [38].

4) *A Sweet Spot for the Past Horizon p* : Assumption 4.1 implies that to make the truncation bias $\tilde{\Theta}_i^B$ decay much faster than the cross-term error $\tilde{\Theta}_i^E$, the past horizon p should increase at a proper rate with N , i.e., $p = \beta \log N$, where β is sufficiently large. Meanwhile, a larger p means that there are more parameters to be estimated, thus implying a larger error bound. This highlights that, for a fixed N , there is a sweet spot for the choice of p . Similar conclusions are found in asymptotic analysis [23], [51], suggesting that p should grow moderately with N , neither too slow nor too fast. In practice though, p can be selected using information criteria or a two-step procedure—either by minimizing the prediction error of the estimated state-space model or by directly minimizing the error bounds. We use the numerical example (47) to demonstrate the existence of the sweet spot. We fix the future horizon at $f = 7$, and vary the number of samples $\bar{N} = 500 : 1000 : 2500$ and the past horizon $p = 2 : 4 : 30$. The input is white, and the weighting matrices are chosen as $W_1 = I$ and $W_2 = I$. We run 100 Monte Carlo trials. The performance is evaluated by the average normalized error of the poles $\|\hat{a} - a\| / \|a\|$, where \hat{a} is obtained using two realization algorithms. As shown in Figure 1, for both two realization methods, when the number of samples is fixed, there is a sweet spot for p that minimizes the errors. In addition, when the number of samples increases, the sweet spot for p tends to increase as well.

5) *On the Impact of Weighting Matrices*: In the asymptotic regime, the impact of weighting matrices is discussed in [18], [19], [24], [25]. At a high level, W_1 is related to a maximum likelihood or CVA objective, while W_2 is related to an orthogonal projection. In addition, W_1 has little impact on the asymptotic accuracy of Γ_f , and W_2 has little impact on the asymptotic accuracy of L_p . As shown in Theorem 5.1, our work provides a new perspective on the impact of weighting matrices. To be specific, for the robustness of SVD, the condition (43) should be satisfied, which guarantees that the singular

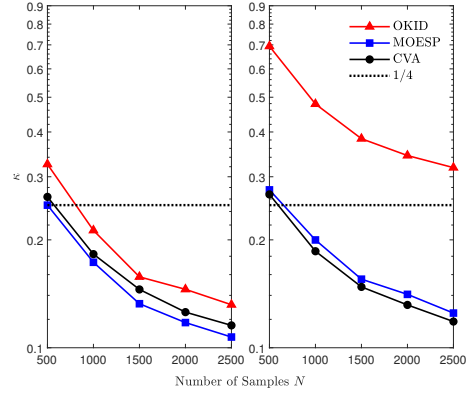


Fig. 2. Robustness condition: white input (left) and colored input (right), where the three curves are from three types of weighting matrices.

vectors related to small singular values of $W_1 \mathcal{H}_{fp} W_2$ can be separated from the singular vectors coming from the noise $W_1 (\hat{\mathcal{H}}_{fp} - \mathcal{H}_{fp}) W_2$. Because W_1 and W_2 reshape these singular values, they can either relax or tighten the condition (43). To see this clearly, we use the numerical example (47) to show the impact of different weighting matrices in Table I. The simulation settings are the same as before, and the past horizon is fixed at $p = f = 7$. Both white input and colored input are considered. The performance is evaluated by the ratio

$$\kappa := \frac{\|W_1(\hat{\mathcal{H}}_{fp} - \mathcal{H}_{fp})W_2\|}{\sigma_{n_x}(W_1 \mathcal{H}_{fp} W_2)}. \quad (48)$$

We determine whether the condition (43) is satisfied or not by comparing κ with $1/4$. The results are shown in Figure 2⁵.

First, Figure 2 suggests that different weighting matrices result in different number of samples required for the condition (43) to be satisfied. Since $\|\hat{\mathcal{H}}_{fp} - \mathcal{H}_{fp}\|$ decays as $\mathcal{O}(1/\sqrt{N})$, no matter what pair of weighting matrices we choose, $\kappa \leq 1/4$ will be eventually satisfied as $N \rightarrow \infty$. However, a good choice of weighting matrices makes it easier to satisfy this condition, such as the MOESP weighting.

Second, both weighting matrices W_1 and W_2 affect the robustness condition. As shown in Figure 2, MOESP and CVA employ different W_1 and the same W_2 , which result in different robustness conditions. Meanwhile, MOESP and OKID employ different W_2 and the same W_1 , which also result in different robustness conditions.

Third, the impact of weighting matrices is input-dependent. As shown in Figure 2, it is easier for the MOESP weighting to satisfy the condition (43) when the input is white than colored.

Fourth, besides their impact on the robustness condition, the weighting matrices also influence the estimation accuracy. It should be emphasized that a pair of weighting matrices making the robustness condition easier to achieve does not mean that they also imply a smaller estimation error. To illustrate this, we choose the estimate of poles coming from two realization algorithms to demonstrate the impact of the weighting matrices. The simulation settings are same as before, and only the

⁵Note that N4SID gives almost identical results as MOESP, and IVM gives almost identical results as CVA, so only results for MOESP, CVA and OKID are presented.

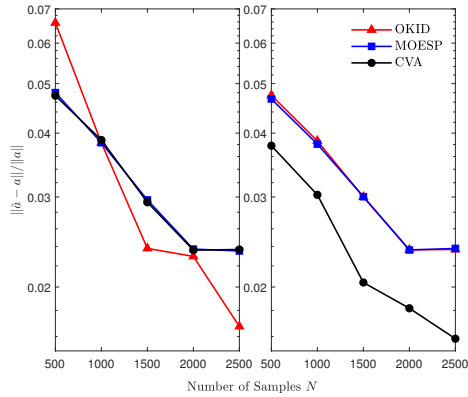


Fig. 3. Normalized error of poles: MOESP (left) and Larimore (right), where the three curves are from three types of weighting matrices⁷.

white input is considered. The performance is evaluated by the normalized error of the poles $\|\hat{a} - a\| / \|a\|$. The results are shown in Figure 3. Based on the right subplots of Figures 2 and 3, we see that compared to the CVA weighting, although the MOESP weighting makes the robustness condition easier to achieve, it increases the estimation error of the poles.

In addition, as shown in Figure 3, W_1 has minor influence on the estimate of the poles for the MOESP type realization, and W_2 has minor influence on the estimate of the poles for the Larimore type realization. This is consistent with an analysis in the asymptotic regime [18], [19], [24], [25]. However, this conclusion cannot be obtained through our finite sample analysis. This comparison underscores the view that both asymptotic and non-asymptotic methods are valuable in uncovering the statistical properties of SIMs, and they complement each other.

Finally, we remark that the robustness condition (43) is a sufficient condition, and our results are upper bounds. It is not sufficient to determine the best choice of weighting matrices solely based on the criteria of facilitating the achievement of robustness conditions and minimizing the upper bounds. To fully grasp the influence of the weighting matrices and develop an optimal choice, further study is needed.

VII. CONCLUSION

This paper presents a finite sample analysis for a large class of open-loop SIMs. Compared with the-state-of-art that mainly analyzes the performance of the Ho-Kalman algorithm or similar variants, we investigate one of the most representative SIMs, PARSIM. Our analysis establishes a more general PE condition, and takes the different weighting matrices and two realization algorithms into account. It not only confirms that the convergence rates for estimating the Markov parameters and system matrices are $\mathcal{O}(1/\sqrt{N})$ even in the presence of inputs, in line with classical asymptotic results, but it also provides high-probability upper bounds for these estimates.

⁷Although the OKID weighting performs better for the MOESP type of realization when N becomes larger in this simple example, it generally does not outperform other methods in most cases. Additionally, since we estimate $\mathcal{H}_{f,p}$ using PARSIM, the best results of OKID is primarily attributable to PARSIM rather than the original OKID approach which estimates $\mathcal{H}_{f,p}$ in a different way [7].

Our findings complement the existing asymptotic results, and methodologies can be similarly applied to many variants of SIMs, such as classical SIMs, SSARX and PBSID.

REFERENCES

- [1] B. L. Ho and R. E. Kálmán, "Effective construction of linear state-variable models from input/output functions," *Automatisierungstechnik*, vol. 14, no. 1-12, pp. 545–548, 1966.
- [2] S. J. Qin, "An overview of subspace identification," *Comput. Chem. Eng.*, vol. 30, no. 10-12, pp. 1502–1513, 2006.
- [3] G. Van der Veen, J.-W. van Wingerden, M. Bergamasco, M. Lovera, and M. Verhaegen, "Closed-loop subspace identification methods: An overview," *IET Control Theory Appl.*, vol. 7, no. 10, pp. 1339–1358, 2013.
- [4] W. E. Larimore, "Canonical variate analysis in identification, filtering and adaptive control," in *Proc. IEEE Conf. Decis. Control*, Honolulu, HI, USA, 1990.
- [5] P. Van Overschee and B. De Moor, "N4SID: Subspace algorithms for the identification of combined deterministic-stochastic systems," *Automatica*, vol. 30, no. 1, pp. 75–93, 1994.
- [6] M. Verhaegen and P. Dewilde, "Subspace model identification part I: the output-error state-space model identification class of algorithm," *Int. J. Control.*, vol. 56, pp. 1187–1210, 1992.
- [7] M. Phan, L. G. Horta, J.-N. Juang, and R. W. Longman, "Improvement of observer/Kalman filter identification (OKID) by residual whitening," in *AIAA Guid., Nav. and Control Conf.*, South Carolina, USA, 1995.
- [8] S. J. Qin, W. Lin, and L. Ljung, "A novel subspace identification approach with enforced causal models," *Automatica*, vol. 41, no. 12, pp. 2043–2053, 2005.
- [9] J. He, C. R. Rojas, and H. Hjalmarsson, "Weighted least-squares PARSIM," in *Proc. 20th IFAC Symp. Syst. Identification*, vol. 58, no. 15, 2024, pp. 330–335.
- [10] M. Deistler, K. Peternell, and W. Scherrer, "Consistency and relative efficiency of subspace methods," *Automatica*, vol. 31, no. 12, pp. 1865–1875, 1995.
- [11] W. E. Larimore, "Statistical optimality and canonical variate analysis system identification," *Signal Process.*, vol. 52, no. 2, pp. 131–144, 1996.
- [12] K. Peternell, W. Scherrer, and M. Deistler, "Statistical analysis of novel subspace identification methods," *Signal Process.*, vol. 52, no. 2, pp. 161–177, 1996.
- [13] M. Jansson and B. Wahlberg, "On consistency of subspace methods for system identification," *Automatica*, vol. 34, no. 12, pp. 1507–1519, 1998.
- [14] D. Bauer, M. Deistler, and W. Scherrer, "Consistency and asymptotic normality of some subspace algorithms for systems without observed inputs," *Automatica*, vol. 35, no. 7, pp. 1243–1254, 1999.
- [15] T. Knudsen, "Consistency analysis of subspace identification methods based on a linear regression approach," *Automatica*, vol. 37, no. 1, pp. 81–89, 2001.
- [16] D. Bauer and M. Jansson, "Analysis of the asymptotic properties of the MOESP type of subspace algorithms," *Automatica*, vol. 36, no. 4, pp. 497–509, 2000.
- [17] M. Jansson, "Asymptotic variance analysis of subspace identification methods," *Proc. 12th IFAC Symp. Syst. Identification*, vol. 33, no. 15, pp. 91–96, 2000.
- [18] T. Gustafsson, "Subspace-based system identification: weighting and pre-filtering of instruments," *Automatica*, vol. 38, no. 3, pp. 433–443, 2002.
- [19] D. Bauer, "Asymptotic properties of subspace estimators," *Automatica*, vol. 41, no. 3, pp. 359–376, 2005.
- [20] A. Chiuso and G. Picci, "The asymptotic variance of subspace estimates," *J. Econom.*, vol. 118, no. 1-2, pp. 257–291, 2004.
- [21] ———, "Consistency analysis of some closed-loop subspace identification methods," *Automatica*, vol. 41, no. 3, pp. 377–391, 2005.
- [22] A. Chiuso, "On the relation between CCA and predictor-based subspace identification," *IEEE Trans. Autom. Control*, vol. 52, no. 10, pp. 1795–1812, 2007.
- [23] ———, "The role of vector autoregressive modeling in predictor-based subspace identification," *Automatica*, vol. 43, no. 6, pp. 1034–1048, 2007.
- [24] D. Bauer, M. Deistler, and W. Scherrer, "On the impact of weighting matrices in subspace algorithms," in *Proc. 12nd IFAC Symp. Syst. Identification*, California, USA, 2000.

[25] D. Bauer and L. Ljung, "Some facts about the choice of the weighting matrices in Larimore type of subspace algorithms," *Automatica*, vol. 38, no. 5, pp. 763–773, 2002.

[26] E. J. Hannan and M. Deistler, *The Statistical Theory of Linear Systems*. SIAM, 2012.

[27] M. C. Campi and E. Weyer, "Finite sample properties of system identification methods," *IEEE Trans. Autom. Control*, vol. 47, no. 8, pp. 1329–1334, 2002.

[28] E. Weyer, R. C. Williamson, and I. M. Mareels, "Finite sample properties of linear model identification," *IEEE Trans. Autom. Control*, vol. 44, no. 7, pp. 1370–1383, 1999.

[29] T. Sarkar and A. Rakhlis, "Near optimal finite time identification of arbitrary linear dynamical systems," in *Int. Conf. on Machine Learn.*, 2019, pp. 5610–5618.

[30] M. Simchowitz, H. Mania, S. Tu, M. I. Jordan, and B. Recht, "Learning without mixing: Towards a sharp analysis of linear system identification," in *Conf. on Learn. Theory*, 2018.

[31] Y. Jedra and A. Proutiere, "Finite-time identification of linear systems: Fundamental limits and optimal algorithms," *IEEE Trans. Autom. Control*, vol. 68, no. 5, pp. 2805 – 2820, 2022.

[32] A. Tsiamis and G. J. Pappas, "Finite sample analysis of stochastic system identification," in *IEEE Conf. Decis. Control*, 2019, pp. 3648–3654.

[33] S. Oymak and N. Ozay, "Non-asymptotic identification of LTI systems from a single trajectory," in *Am. Control Conf.*, 2019, pp. 5655–5661.

[34] M. Simchowitz, R. Boczar, and B. Recht, "Learning linear dynamical systems with semi-parametric least squares," in *Conf. on Learn. Theory*, 2019, pp. 2714–2802.

[35] T. Sarkar, A. Rakhlis, and M. A. Dahleh, "Finite time LTI system identification," *J. Mach. Learn. Res.*, vol. 22, no. 1, pp. 1186–1246, 2021.

[36] S. Lale, K. Azizzadenesheli, B. Hassibi, and A. Anandkumar, "Finite-time system identification and adaptive control in autoregressive exogenous systems," in *Learn. Dyn. Control*, 2021, pp. 967–979.

[37] A. Bakshi, A. Liu, A. Moitra, and M. Yau, "A new approach to learning linear dynamical systems," in *Proc. 55th Annual ACM Symp. on Theory of Computing*, 2023, pp. 335–348.

[38] A. Tsiamis, I. Ziemann, N. Matni, and G. J. Pappas, "Statistical learning theory for control: A finite-sample perspective," *IEEE Control Syst.*, vol. 43, no. 6, pp. 67–97, 2023.

[39] S. Sun, J. Li, and Y. Mo, "Finite time performance analysis of MIMO systems identification," *arXiv preprint arXiv:2310.11790*, 2023.

[40] M. Jansson, "Subspace identification and ARX modeling," in *Proc. 13th IFAC Symp. Syst. Identification*, Netherlands, 2003.

[41] J. He, I. Ziemann, C. R. Rojas, and H. Hjalmarsson, "Finite sample analysis for a class of subspace identification methods," *arXiv preprint arXiv:2404.17331*, 2024.

[42] I. Ziemann, A. Tsiamis, B. Lee, Y. Jedra, N. Matni, and G. J. Pappas, "A tutorial on the non-asymptotic theory of system identification," in *IEEE Conf. Decis. and Control*, 2023, pp. 8921–8939.

[43] L. Ljung, *System identification: Theory for the user*. Prentice Hall information and system sciences series, Prentice Hall PTR, 1999.

[44] P. Van Overschee and B. De Moor, *Subspace identification for linear systems: Theory-Implementation- Applications*. Springer, 2012.

[45] S. Oymak and N. Ozay, "Revisiting Ho-Kalman-based system identification: Robustness and finite-sample analysis," *IEEE Trans. Autom. Control*, vol. 67, no. 4, pp. 1914–1928, 2021.

[46] P. Van Overschee and B. De Moor, "A unifying theorem for three subspace system identification algorithms," *Automatica*, vol. 31, no. 12, pp. 1853–1864, 1995.

[47] M. Verhaegen, "Identification of the deterministic part of MIMO state space models given in innovations form from input-output data," *Automatica*, vol. 30, no. 1, pp. 61–74, 1994.

[48] M. Viberg, "Subspace-based methods for the identification of linear time-invariant systems," *Automatica*, vol. 31, no. 12, pp. 1835–1851, 1995.

[49] S. Tu, R. Boczar, M. Simchowitz, M. Soltanolkotabi, and B. Recht, "Low-rank solutions of linear matrix equations via procrustes flow," in *Int. Conf. on Machine Learn.* PMLR, 2016, pp. 964–973.

[50] I. Ziemann, "A note on the smallest eigenvalue of the empirical covariance of causal Gaussian processes," *IEEE Trans. Autom. Control*, vol. 69, no. 2, pp. 1372–1376, 2023.

[51] M. Galrinho, C. R. Rojas, and H. Hjalmarsson, "Parametric identification using weighted null-space fitting," *IEEE Trans. Autom. Control*, vol. 64, no. 7, pp. 2798–2813, 2018.

[52] Y. Abbasi-Yadkori and C. Szepesvári, "Regret bounds for the adaptive control of linear quadratic systems," in *Conf. on Learn. Theory*, 2011, pp. 1–26.

[53] J. A. Tropp, "User-friendly tail bounds for sums of random matrices," *Found. Comput. Math.*, vol. 12, pp. 389–434, 2012.

[54] T. Tao, "254a, notes 3a: Eigenvalues and sums of Hermitian matrices," 2010. [Online]. Available: <https://terrytao.wordpress.com/2010/01/12/254a-notes-3a-eigenvalues-and-sums-of-hermitian-matrices/>

[55] R. Ahlsweide and A. Winter, "Strong converse for identification via quantum channels," *IEEE Trans. Inf. Theory*, vol. 48, no. 3, pp. 569–579, 2002.

[56] Y. Abbasi-Yadkori, D. Pál, and C. Szepesvári, "Online least squares estimation with self-normalized processes: An application to bandit problems," *arXiv preprint arXiv:1102.2670*, 2011.

[57] D. L. Hanson and F. T. Wright, "A bound on tail probabilities for quadratic forms in independent random variables," *Ann. Math. Stat.*, vol. 42, no. 3, pp. 1079–1083, 1971.

[58] P.-Å. Wedin, "Perturbation theory for pseudo-inverses," *BIT Numerical Mathematics*, vol. 13, pp. 217–232, 1973.

APPENDIX I BURN-IN TIME AND PERSISTENCE OF EXCITATION

A. Proof of Lemma 1

Based on (31), we have that

$$N\hat{\Sigma}_{p,i,N} = \mathcal{O}_{p,i}X_{k-p}X_{k-p}^\top\mathcal{O}_{p,i}^\top + \mathcal{T}_{p,i}\Lambda_{u,e}W_{p,i}W_{p,i}^\top\Lambda_{u,e}^\top\mathcal{T}_{p,i}^\top + \mathcal{O}_{p,i}X_{k-p}W_{p,i}^\top\Lambda_{u,e}^\top\mathcal{T}_{p,i}^\top + \mathcal{T}_{p,i}\Lambda_{u,e}W_{p,i}X_{k-p}^\top\mathcal{O}_{p,i}^\top. \quad (\text{I.1})$$

In the following, we use a three-step procedure to show that $\hat{\Sigma}_{p,i,N}$ is invertible with high probability.

Step 1 (Noises and inputs PE): Here we establish the PE condition for the corrections of noises and inputs, i.e., the term $\mathcal{T}_{p,i}\Lambda_{u,e}W_{p,i}W_{p,i}^\top\Lambda_{u,e}^\top\mathcal{T}_{p,i}^\top$. Since $\mathcal{T}_{p,i}\Lambda_{u,e}$ is a full-row rank matrix, we mainly show that the following event occurs with high probability:

$$\mathcal{E}_{i,W} = \left\{ W_{p,i}W_{p,i}^\top = \sum_{k=1}^N w_{p,i}(k)w_{p,i}^\top(k) \succcurlyeq \frac{N}{2}I \right\}. \quad (\text{I.2})$$

Since $W_{p,i}$ contains two block Hankel matrices, existing lower bounds on individual Hankel matrices in [32], [45] cannot be directly used. We propose another approach to bound it. Based on (28), we have $\mathbb{E}[w_{p,i}(k)w_{p,i}^\top(k)] = I$, which further gives

$$\sigma_{\min}(\mathbb{E}[w_{p,i}(k)w_{p,i}^\top(k)]) = 1. \quad (\text{I.3})$$

We now provide a upper bound for $\|w_{p,i}(k)\|$. Since $e_k \sim \mathcal{N}(0, I)$ and $u_k \sim \mathcal{N}(0, \sigma_u^2 I)$, we conclude that u_k and e_k are component-wise sub-Gaussian random variables with variance σ_u^2 and 1, respectively. Therefore, for all $1 \leq k \leq N$, with probability at least $1 - \delta$, we have

$$\sigma_u^{-1}\|u_k\| \leq \bar{u} := n_u \sqrt{2n_u \log(\frac{32n_u N}{\delta})}, \quad (\text{I.4a})$$

$$\|e_k\| \leq \bar{e} := n_y \sqrt{2n_y \log(\frac{32n_y N}{\delta})}. \quad (\text{I.4b})$$

Furthermore, it is straightforward to see that

$$\|w_{p,i}(k)\| \leq \bar{w}_{p,i} := \bar{e}\sqrt{p} + \bar{u}\sqrt{p+i}. \quad (\text{I.5})$$

We now define

$$r_{p,i}(k) = w_{p,i}(k)w_{p,i}^\top(k) - \mathbb{E}[w_{p,i}(k)w_{p,i}^\top(k)], \quad (\text{I.6a})$$

$$R_{p,i} = \sum_{k=1}^N r_{p,i}(k), \quad (\text{I.6b})$$

and their truncation

$$\tilde{r}_{p,i}(k) = r_{p,i}(k) \mathbb{I}_{\{r_{p,i}(k) \leq 2\bar{w}_{p,i}^2 I\}}, \quad (\text{I.7a})$$

$$\tilde{R}_{p,i} = \sum_{k=1}^N \tilde{r}_{p,i}(k). \quad (\text{I.7b})$$

Further, we define a upper bound $\bar{r}_{p,i} = 2\bar{w}_{p,i}^2 \sqrt{2\log(\frac{d_i}{\delta})}$. According to Lemma 9, we have

$$\begin{aligned} \mathbb{P}\left(R_{p,i} \succ \bar{r}_{p,i} \sqrt{NI}\right) &\leq \mathbb{P}\left(\tilde{R}_{p,i} \succ \bar{r}_{p,i} \sqrt{NI}\right) + \\ &\quad \mathbb{P}\left(\max_{1 \leq k \leq N} r_{p,i}(k) \succ 2\bar{w}_{p,i}^2 I\right). \end{aligned} \quad (\text{I.8})$$

Based on Lemma 10 and (I.5), each term on the right hand side of (I.8) is bounded by δ . Thus, with probability of at least $1 - 2\delta$, we have

$$\lambda_{\max}(R_{p,i}) \leq \bar{r}_{p,i} \sqrt{N}. \quad (\text{I.9})$$

Combining (I.3) and (I.9), and using Weyl's inequality in Lemma 11, we have that with probability at least $1 - 2\delta$,

$$\sigma_{\min}\left(\sum_{k=1}^N w_{p,i}(k) w_{p,i}^\top(k)\right) \geq N - \bar{r}_{p,i} \sqrt{N}. \quad (\text{I.10})$$

Define

$$N_W(\delta, p, i) := 4\bar{r}_{p,i}^2. \quad (\text{I.11})$$

For $N \geq N_W(\delta, p, i)$, we then have that with probability at least $1 - 2\delta$,

$$\sigma_{\min}\left(\sum_{k=1}^N w_{p,i}(k) w_{p,i}^\top(k)\right) \geq \frac{N}{2} > 0. \quad (\text{I.12})$$

Step 2 (Cross terms are small): We now show that the cross term $\mathcal{O}_{p,i} X_{k-p} W_{p,i}^\top \Lambda_{u,e}^\top \mathcal{T}_{p,i}^\top$ is much smaller and its norm increases with a rate of at most $\mathcal{O}(\sqrt{N})$ up to logarithmic terms. We first use the Markov inequality in Lemma 12 to upper bound state correlations $X_{k-p} X_{k-p}^\top$, which states that the following event holds with probability $1 - \frac{\delta}{2}$:

$$\mathcal{E}_{i,X} := \left\{ X_{k-p} X_{k-p}^\top \preccurlyeq N \frac{2n_x}{\delta} \Sigma_{x,N} \right\}. \quad (\text{I.13})$$

Using Lemma 13 we have that with probability $1 - \frac{\delta}{2}$:

$$\begin{aligned} \left\| (X_{k-p} X_{k-p}^\top + NI)^{-\frac{1}{2}} X_{k-p} W_{p,i}^\top \right\|^2 &\leq \\ 4\log \frac{\det(X_{k-p} X_{k-p}^\top + NI)}{\det(NI)} + 8\log \frac{5^{d_i} 2}{\delta} &\quad (\text{I.14}) \end{aligned}$$

Furthermore, conditioned on $\mathcal{E}_{i,X}$, inequality in (I.14) can be relaxed to that with probability $1 - \delta$:

$$\mathcal{E}_{i,XE} := \left\{ \left\| (X_{k-p} X_{k-p}^\top + NI)^{-\frac{1}{2}} X_{k-p} W_{p,i}^\top \right\|^2 \leq C_{i,XE} \right\}, \quad (\text{I.15})$$

where $C_{i,XE} = 4\log(\det(I + \frac{2n_x}{\delta} \Sigma_{x,N})) + 8\log \frac{5^{d_i} 2}{\delta}$. In this way, we have that with probability $1 - \delta$,

$$\left\| X_{k-p} W_{p,i}^\top \right\| \leq \left\| (X_{k-p} X_{k-p}^\top + NI)^{\frac{1}{2}} \right\| \sqrt{C_{i,XE}}, \quad (\text{I.16})$$

which implies that $\mathcal{O}_{p,i} X_{k-p} W_{p,i}^\top \Lambda_{u,e}^\top \mathcal{T}_{p,i}^\top$ increases at most $\mathcal{O}(\sqrt{N})$ up to logarithmic terms.

Step 3 (Inputs and outputs PE): From Steps 1 and 2, we summarize that for $N \geq N_W(N, \delta, p, i)$, the event $\mathcal{E}_{i,W} \cap \mathcal{E}_{i,XE}$ occurs with probability at least $1 - 3\delta$. In this step, we show that if the number of samples is large enough, then,

$$N \hat{\Sigma}_{p,i,N} \succcurlyeq \mathcal{O}_{p,i} X_{k-p} X_{k-p}^\top \mathcal{O}_{p,i}^\top + \mathcal{T}_{p,i} \Lambda_{u,e} W_{p,i} W_{p,i}^\top \Lambda_{u,e}^\top \mathcal{T}_{p,i}^\top,$$

holds with high probability. For an arbitrary unit vector $v \in \mathbb{R}^{d_i}$, we define

$$\alpha_i := \frac{1}{N} v^\top \mathcal{O}_{p,i} X_{k-p} X_{k-p}^\top \mathcal{O}_{p,i}^\top v, \quad (\text{I.17a})$$

$$\beta_i := \frac{1}{N} v^\top \mathcal{T}_{p,i} \Lambda_{u,e} W_{p,i} W_{p,i}^\top \Lambda_{u,e}^\top \mathcal{T}_{p,i}^\top v, \quad (\text{I.17b})$$

$$\gamma_{i,N} := 2 \|\mathcal{T}_{p,i}\| \|\Lambda_{u,e}\| \sqrt{\frac{C_{i,XE}}{N}}. \quad (\text{I.17c})$$

Then, from (I.1), we have that

$$\begin{aligned} v^\top \hat{\Sigma}_{p,i,N} v &= \alpha_i + \beta_i + 2v^\top \mathcal{O}_p X_{k-p} W_{p,i}^\top \Lambda_{u,e}^\top \mathcal{T}_{p,i}^\top v \\ &\geq \alpha_i + \beta_i - \gamma_{i,N} \sqrt{1 + \alpha_i}, \end{aligned}$$

where the second inequality is due to (I.16). Moreover, the event $\mathcal{E}_{i,W}$ implies that $\beta_i \geq \frac{\|\mathcal{T}_{p,i}\|^2 \|\Lambda_{u,e}\|^2}{2} > 0$. Let $N_\Phi(\delta, p, i)$ be such that

$$N_\Phi(\delta, p, i) := \min \{N : \gamma_{i,N} \leq \min \{1, \bar{\sigma}_{p,i}^2\}\}. \quad (\text{I.18})$$

Since $C_{i,XE}$ grows at most logarithmically with N , $N_\Phi(\delta, p, i)$ always exist. Using Lemma 20, we conclude that with probability at least $1 - 3\delta$:

$$\alpha_i + \beta_i - \gamma_{i,N} \sqrt{1 + \alpha_i} \geq \frac{\alpha_i + \beta_i}{2} \geq \frac{\beta_i}{2}, \quad (\text{I.19})$$

$$\text{where } \frac{\beta_i}{2} = \frac{\|\mathcal{T}_{p,i}\|^2 \|\Lambda_{u,e}\|^2}{4} := \bar{\sigma}_{p,i}^2. \quad \blacksquare$$

APPENDIX II BOUND ON CROSS-TERM ERROR

A. Proof of Lemma 2

To bound the cross-term error $\tilde{\Theta}_i^E$, we first define the following three events, where each of them occurs with probability at least $1 - \delta/3$:

$$\mathcal{E}_{i,\Phi_1} := \left\{ \hat{\Sigma}_{p,i,N} \succcurlyeq \bar{\sigma}_{p,i}^2 I \right\},$$

$$\mathcal{E}_{i,\Phi_2} := \left\{ \hat{\Sigma}_{p,i,N} \preccurlyeq \frac{3d_{p,i}}{\delta} \Sigma_{p,i,N} \right\},$$

$$\mathcal{E}_{i,\Phi_3} := \left\{ \left\| \sum_{k=1}^N e_i(k) \phi_{p,i}(k)^\top \left(\Sigma + N \hat{\Sigma}_{p,i,N} \right)^{-\frac{1}{2}} \right\|^2 \leq 4\log \frac{\det(\Sigma + N \hat{\Sigma}_{p,i,N})}{\det(\Sigma)} + 8 \left(\log \frac{5^{n_y} 3}{\delta} \right) \right\},$$

where matrix $\Sigma \succ 0$. The event \mathcal{E}_{i,Φ_1} is due to the PE condition in Lemma 1, the event \mathcal{E}_{i,Φ_2} is derived from an extension of Markov's inequality in Lemma 12, and the event \mathcal{E}_{i,Φ_3} is based on self-normalized martingales in Lemma 13.

The main idea is to show that the event in Lemma 2 is subsumed by the intersection of events \mathcal{E}_{i,Φ_1} , \mathcal{E}_{i,Φ_2} and \mathcal{E}_{i,Φ_3} , with $\mathbb{P}\left(\bigcap_{j=1}^3 \mathcal{E}_{i,\Phi_j}\right) \geq 1 - \delta$. According to (32), we have that

$$\begin{aligned} \left\|\tilde{\Theta}_i^E\right\|^2 &= \left\|\left(H_{fi} \sum_{k=1}^N \frac{1}{N} e_i(k) \phi_{p,i}^\top(k) \hat{\Sigma}_{p,i,N}^{-\frac{1}{2}}\right) \hat{\Sigma}_{p,i,N}^{-\frac{1}{2}}\right\|^2 \\ &\leq \underbrace{\left\|H_{fi} \sum_{k=1}^N \frac{1}{N} e_i(k) \phi_{p,i}^\top(k) \hat{\Sigma}_{p,i,N}^{-\frac{1}{2}}\right\|^2}_{\text{noise term}} \underbrace{\left\|\hat{\Sigma}_{p,i,N}^{-\frac{1}{2}}\right\|}_{\text{excitation term}}. \end{aligned}$$

The excitation term is bounded based on the event \mathcal{E}_{i,Φ_1} , i.e.,

$$\left\|\hat{\Sigma}_{p,i,N}^{-\frac{1}{2}}\right\| \leq 1/\bar{\sigma}_{p,i}^2. \quad (\text{II.1})$$

Due to \mathcal{E}_{i,Φ_1} , we have $2N\hat{\Sigma}_{p,i,N} \succcurlyeq N\hat{\Sigma}_{p,i,N} + N\bar{\sigma}_{p,i}^2 I$. After substituting it into the noise term, we have

$$\begin{aligned} &\left\|\frac{H_{fi}}{\sqrt{N}} \sum_{k=1}^N e_i(k) \phi_{p,i}^\top(k) \left(N\hat{\Sigma}_{p,i,N}\right)^{-\frac{1}{2}}\right\|^2 \leq \\ &\frac{2\|H_{fi}\|^2}{N} \left\|\sum_{k=1}^N e_i(k) \phi_{p,i}^\top(k) \left(N\bar{\sigma}_{p,i}^2 I + N\hat{\Sigma}_{p,i,N}\right)^{-\frac{1}{2}}\right\|^2. \end{aligned}$$

Taking $\Sigma = N\bar{\sigma}_{p,i}^2 I$ in \mathcal{E}_{i,Φ_3} , the noise term is relaxed to

$$\begin{aligned} &\left\|\sum_{k=1}^N e_i(k) \phi_{p,i}^\top(k) \left(N\bar{\sigma}_{p,i}^2 I + N\hat{\Sigma}_{p,i,N}\right)^{-\frac{1}{2}}\right\|^2 \leq \\ &4\log \frac{\det(N\bar{\sigma}_{p,i}^2 I + N\hat{\Sigma}_{p,i,N})}{\det(N\bar{\sigma}_{p,i}^2 I)} + 8\left(\log \frac{5^{n_y} 3}{\delta}\right) \leq \\ &4\log \left(\det(I + \frac{3d_{p,i}}{\delta\bar{\sigma}_{p,i}^2} \Sigma_{p,i,N})\right) + 8\left(\log \frac{5^{n_y} 3}{\delta}\right) \leq \\ &4\left(d_{p,i} \log \frac{6d_{p,i}}{\delta} + \log \left(\det(\frac{\Sigma_{p,i,N}}{\bar{\sigma}_{p,i}^2})\right) + 2\left(\log \frac{5^{n_y} 3}{\delta}\right)\right), \end{aligned} \quad (\text{II.2})$$

where the second inequality is due to \mathcal{E}_{i,Φ_2} , and the third inequality is due to $I \preccurlyeq \frac{3d_{p,i}}{\bar{\sigma}_{p,i}^2} \Sigma_{p,i,N}$ under \mathcal{E}_{i,Φ_1} and \mathcal{E}_{i,Φ_2} . Combining (II.1) and (II.2), and absorbing minor terms by inflating the constants c_1 accordingly, we have

$$\left\|\tilde{\Theta}_i^E\right\|^2 \leq c_1 \frac{\epsilon_{i,E}^2}{N},$$

where $\epsilon_{i,E}^2 = \frac{\|H_{fi}\|^2}{\bar{\sigma}_{p,i}^2} \left(d_{p,i} \log \frac{d_{p,i}}{\delta} + \log \left(\det(\frac{\Sigma_{p,i,N}}{\bar{\sigma}_{p,i}^2})\right)\right)$. ■

APPENDIX III

BOUND ON TRUNCATION BIAS

To prove Lemma 3, we need the following auxiliary lemma:

Lemma 5: Fix a failure probability $0 < \delta < 1$. There exists a universal constant $c_2 \geq 16\sqrt{2} + \frac{1}{\log \frac{2}{\delta}}$, such that with probability at least $1 - \delta$,

$$\sum_{k=1}^N \|x_k\|^2 \leq c_2 n_x N \|\Sigma_{x,N}\| \log \frac{2}{\delta}. \quad (\text{III.1})$$

Proof: The proof is identical to Lemma E.5 in [42], which is an application of Hanson-Wright inequality in Lemma 14, thus, it is omitted here. ■

A. Proof of Lemma 3

The bias term $\tilde{\Theta}_i^B$ can be similarly decomposed as

$$\tilde{\Theta}_i^B = \left(\Gamma_{fi} A_K^p \sum_{k=1}^N x_k \phi_{p,i}^\top(k) (N\hat{\Sigma}_{p,i,N})^{-\frac{1}{2}}\right) (N\hat{\Sigma}_{p,i,N})^{-\frac{1}{2}}.$$

Note that $N\hat{\Sigma}_{p,i,N} = \sum_{j=1}^N \phi_{p,i}(j) \phi_{p,i}^\top(j) \succcurlyeq \phi_{p,i}(k) \phi_{p,i}^\top(k)$ for each k , hence, by the Schur complement, we have

$$\phi_{p,i}^\top(k) (N\hat{\Sigma}_{p,i,N})^{-1} \phi_{p,i}(k) \leq 1. \quad (\text{III.2})$$

Using the triangle inequality, we have

$$\begin{aligned} &\left\|\sum_{k=1}^N x_k \phi_{p,i}^\top(k) (N\hat{\Sigma}_{p,i,N})^{-\frac{1}{2}}\right\| \leq \\ &\sum_{k=1}^N \|x_k\| \left\|\phi_{p,i}^\top(k) (N\hat{\Sigma}_{p,i,N})^{-\frac{1}{2}}\right\|. \end{aligned} \quad (\text{III.3})$$

Combining (III.2) with (III.3), and using the Cauchy-Schwarz inequality, we further have

$$\left\|\sum_{k=1}^N x_k \phi_{p,i}^\top(k) (N\hat{\Sigma}_{p,i,N})^{-\frac{1}{2}}\right\| \leq \sqrt{N \sum_{k=1}^N \|x_k\|^2}. \quad (\text{III.4})$$

Using inequality (III.1), inequality (III.4) is further relaxed to

$$\left\|\sum_{k=1}^N x_k \phi_{p,i}^\top(k) (N\hat{\Sigma}_{p,i,N})^{-\frac{1}{2}}\right\| \leq \sqrt{c_2 n_x \|\Sigma_{x,N}\| N^2 \log \frac{1}{\delta}}. \quad (\text{III.5})$$

Combining (II.1) and (III.5), the bias term is bounded by

$$\left\|\tilde{\Theta}_i^B\right\|^2 \leq \frac{c_2 n_x}{\bar{\sigma}_{p,i}^2} \|\Gamma_{fi} A_K^p\| \|\Sigma_{x,N}\| N \log \frac{1}{\delta}. \quad (\text{III.6})$$

Under Assumption 4.1, $\|\Gamma_{fi} A_K^p\| \|\Sigma_{x,N}\| \leq N^{-3}$, then, the bias error is finally bounded by

$$\left\|\tilde{\Theta}_i^B\right\|^2 \leq c_2 \frac{\epsilon_{i,B}^2}{N^2},$$

where $\epsilon_{i,B}^2 = \frac{n_x}{\bar{\sigma}_{p,i}^2} \log \frac{1}{\delta}$. ■

APPENDIX IV WEIGHTED SINGULAR VALUE DECOMPOSITION

To prove Lemma 4 and Theorem 5.1, we first introduce the following auxiliary lemmas:

Lemma 6 ([45, Lemma 5]): Fix a failure probability $\delta_u := (2(N+f-1)n_u)^{-\log^2(2f n_u) \log(2(N+f-1)n_u)}$. There exists a universal constant c_3 such that if $N \geq 2c_3 f n_y \log(1/\delta_u)$, then with probability at least $1 - \delta_u$, we have $\frac{1}{N} U_f U_f^\top \succcurlyeq \frac{1}{2} \sigma_u^2 I$.

Lemma 7: Fix a failure probability $0 < \delta < 1$. Then, with probability at least $1 - 3\delta/2$, we have

$$\bar{\sigma}_{p,0}^2 I \preccurlyeq \hat{\Sigma}_{p,0,N} := \frac{1}{N} Z_p Z_p^\top \preccurlyeq \frac{3d_{p,0}}{\delta} \Sigma_{p,0,N}, \quad (\text{IV.1})$$

where $\bar{\sigma}_{p,0} := \frac{\|\mathcal{T}_{p,0}\| \|\Lambda_{u,e}\|}{2} > 0$, $\mathcal{T}_{p,0} = \begin{bmatrix} G_p & H_p \\ I & 0 \end{bmatrix}$, $d_{p,0} = p(n_x + n_y)$, $\Sigma_{p,0,k} = \mathbb{E}[\phi_{p,0}(k) \phi_{p,0}^\top(k)]$, $\phi_{p,0}(k) = \begin{bmatrix} y_p(k) \\ u_p(k) \end{bmatrix}$.

Proof: The proof for the lower bound is identical to the PE condition in Lemma 1 by taking $i = 0$. Meanwhile, the proof for the upper bound is derived from an extension of Markov's inequality in Lemma 12. For space consideration, they are omitted here. ■

A. Proof of Lemma 4 (Properties of Weighting Matrices)

Since $W_2 = \left(\frac{1}{N}Z_p\Pi_{U_f}^\perp Z_p^\top\right)^{\frac{1}{2}}$, it is equivalent to prove that $\frac{1}{N}Z_p\Pi_{U_f}^\perp Z_p^\top = \frac{1}{N}Z_pZ_p^\top - \frac{1}{N}Z_pU_f^\top(U_fU_f^\top)^{-1}U_fZ_p^\top$ has the same properties as in Lemma 4. A prerequisite is that $\frac{1}{N}U_fU_f^\top \succ 0$, which is guaranteed by Lemma 6.

First, we prove that $\frac{1}{N}Z_p\Pi_{U_f}^\perp Z_p^\top$ is positive definite. According to the second statement on the Schur complement in Lemma 16, $\frac{1}{N}Z_p\Pi_{U_f}^\perp Z_p^\top \succ 0$ is equivalent to requiring

$$\frac{1}{N} \begin{bmatrix} Z_pZ_p^\top & Z_pU_f^\top \\ U_fZ_p^\top & U_fU_f^\top \end{bmatrix} = \hat{\Sigma}_{p,f,N} \succ 0,$$

which is essentially the PE condition in (34) by taking $i = f$.

Second, we prove that $\left\| \frac{1}{N}Z_p\Pi_{U_f}^\perp Z_p^\top \right\|$ grows at most logarithmically with N . According to Lemma 7, we have

$$\frac{1}{N}Z_p\Pi_{U_f}^\perp Z_p^\top \preceq \frac{1}{N}Z_pZ_p^\top \preceq \frac{3d_{p,0}}{\delta} \Sigma_{p,0,N}.$$

As a consequence of Lemma 19, $\|\Sigma_{p,0,N}\|$ grows at most logarithmically with N , we therefore conclude that $\left\| \frac{1}{N}Z_p\Pi_{U_f}^\perp Z_p^\top \right\|$ grows at most logarithmically with N .

Third, we prove that $\left\| \left(\frac{1}{N}Z_p\Pi_{U_f}^\perp Z_p^\top \right)^{-1} \right\|$ is bounded, which is equivalent to showing that the minimal eigenvalue of $\frac{1}{N}Z_p\Pi_{U_f}^\perp Z_p^\top$ is lower bounded. According to the fourth statement of Lemma 16, we have $\lambda_{\min}(\hat{\Sigma}_{p,f,N}) \leq \lambda_{\min}(\frac{1}{N}Z_p\Pi_{U_f}^\perp Z_p^\top)$. Meanwhile, a lower bound on the minimal eigenvalue of $\hat{\Sigma}_{p,f,N}$ has been given in Lemma 1 by taking $i = f$, thus, $\left\| \left(\frac{1}{N}Z_p\Pi_{U_f}^\perp Z_p^\top \right)^{-1} \right\|$ is bounded. ■

B. Proof of Theorem 5.1 (Weighted SVD)

According to Lemma 17 (let $M = W_1\mathcal{H}_{fp}W_2$ and $\hat{M} = W_1\hat{\mathcal{H}}_{fp}W_2$), if condition (43) is satisfied, we have

$$\begin{aligned} \left\| \hat{L}_p - T^\top \bar{L}_p \right\| &= \left\| \hat{\Lambda}_1^{\frac{1}{2}} \hat{V}_1^\top W_2^{-1} - T^\top \Lambda_1^{\frac{1}{2}} V_1^\top W_2^{-1} \right\| \\ &\leq \left\| \hat{\Lambda}_1^{\frac{1}{2}} \hat{V}_1^\top - T^\top \Lambda_1^{\frac{1}{2}} V_1^\top \right\| \left\| W_2^{-1} \right\| \\ &\leq \sqrt{\frac{40n_x}{\sigma_{n_x}(W_1\mathcal{H}_{fp}W_2)}} \left\| W_1 (\hat{\mathcal{H}}_{fp} - \mathcal{H}_{fp}) W_2 \right\| \left\| W_2^{-1} \right\| \\ &\leq \sqrt{\frac{40n_x}{\sigma_{n_x}(W_1\mathcal{H}_{fp}W_2)}} \left\| \hat{\mathcal{H}}_{fp} - \mathcal{H}_{fp} \right\| \left\| W_1 \right\| \left\| W_2 \right\| \left\| W_2^{-1} \right\| \\ &\leq \sqrt{\frac{40n_x}{\sigma_{n_x}(\mathcal{H}_{fp})}} \left\| \hat{\mathcal{H}}_{fp} - \mathcal{H}_{fp} \right\| \frac{\left\| W_1 \right\| \left\| W_2 \right\| \left\| W_2^{-1} \right\|}{\sqrt{\sigma_{\min}(W_2)\sigma_{\min}(W_1)}} \\ &= \sqrt{\frac{40n_x}{\sigma_{n_x}(\mathcal{H}_{fp})}} \left\| \hat{\mathcal{H}}_{fp} - \mathcal{H}_{fp} \right\| W_L, \end{aligned}$$

where W_L are given in (44). The first and third inequalities are due to the triangle inequality, the second inequality is due to Lemma 17, the fourth inequality is due to the relation $\sigma_{n_x}(W_1\mathcal{H}_{fp}W_2) \geq \sigma_{\min}(W_1)\sigma_{n_x}(\mathcal{H}_{fp})\sigma_{\min}(W_2)$, where the rank of \mathcal{H}_{fp} is n_x , and the last equality is due to $\sigma_{\min}(W_2)\sigma_{\min}(W_1) = \left\| W_2^{-1} \right\|^{-1} \left\| W_1^{-1} \right\|^{-1}$. The bound of $\left\| \hat{\Gamma}_f - \bar{\Gamma}_f T \right\|$ can be similarly derived. ■

APPENDIX V

BOUNDS ON SYSTEM MATRICES

A. Proof of Theorem 5.2 (CVA Type Realization)

1) *Bound on C* : To estimate C , we first rewrite (23a) as

$$\begin{aligned} Y_{f1} &= \bar{C}TT^\top \bar{X}_k + \Sigma_e^{1/2}E_{f1} \\ &= \bar{C}T\hat{X}_k + \bar{C}T(T^\top \bar{X}_k - \hat{X}_k) + \Sigma_e^{1/2}E_{f1}. \end{aligned}$$

According to (25a), the estimate of C is $\hat{C} = Y_{f1}\hat{X}_k^\dagger$, where $\hat{X}_k^\dagger = Z_p^\top \hat{L}_p^\top (\hat{L}_p Z_p Z_p^\top \hat{L}_p^\top)^{-1}$. In this way, the estimation error of C can be decomposed into three types:

$$\begin{aligned} \tilde{C} &:= \hat{C} - \bar{C}T = \bar{C}T(T^\top \bar{X}_k - \hat{X}_k)\hat{X}_k^\dagger + \Sigma_e^{1/2}E_{f1}\hat{X}_k^\dagger \\ &= \tilde{C}^L + \tilde{C}^B + \tilde{C}^E, \end{aligned} \quad (\text{V.1})$$

where

$$\begin{aligned} \tilde{C}^L &:= \bar{C}T(T^\top \bar{L}_p - \hat{L}_p)Z_p\hat{X}_k^\dagger, \\ \tilde{C}^B &:= CA_K^p X_{k-p}\hat{X}_k^\dagger, \\ \tilde{C}^E &:= \Sigma_e^{1/2}E_{f1}\hat{X}_k^\dagger. \end{aligned}$$

First, we rewrite the error coming from \hat{L}_p as

$$\tilde{C}^L = \bar{C}T(T^\top \bar{L}_p - \hat{L}_p)Z_p Z_p^\top \hat{L}_p^\top (\hat{L}_p Z_p Z_p^\top \hat{L}_p^\top)^{-1}.$$

For convenience, we define

$$\text{Cond}(\Phi_{p,0}\Phi_{p,0}) = \hat{L}_p Z_p Z_p^\top \hat{L}_p^\top (\hat{L}_p Z_p Z_p^\top \hat{L}_p^\top)^{-1},$$

where $\Phi_{p,0} = Z_p$. Using Lemma 7, we have that

$$\left\| \text{Cond}(\Phi_{p,0}\Phi_{p,0}) \right\| \leq \frac{\left\| \hat{L}_p \right\|^2}{\sigma_{\min}^2(\hat{L}_p)} \frac{\left\| \Sigma_{p,0,N} \right\|}{\sigma_{p,0}^2} \frac{3d_{p,0}}{\delta},$$

which grows at most logarithmically with N . In this way, we have that

$$\left\| \tilde{C}^L \right\| \leq c_4 \left\| \hat{L}_p - T^\top \bar{L}_p \right\|, \quad (\text{V.2})$$

where $c_4 := \left\| \bar{C}T \right\| \left\| \text{Cond}(\Phi_{p,0}\Phi_{p,0}) \right\|$.

Second, the truncation bias can be rewritten as

$$\begin{aligned} \tilde{C}^B &= CA_K^p X_{k-p} Z_p^\top \hat{L}_p^\top (\hat{L}_p Z_p Z_p^\top \hat{L}_p^\top)^{-1} \\ &= CA_K^p X_{k-p} Z_p^\top (Z_p Z_p^\top)^{-1} \text{Cond}(\Phi_{p,0}\Phi_{p,0}). \end{aligned}$$

Similar to bounding $\tilde{\Theta}_i^B$ in Lemma 3, by taking $i = 0$, \tilde{C}^B is bounded by

$$\left\| \tilde{C}^B \right\|^2 \leq \frac{c_5 \epsilon_{0,B}^2}{N^2}, \quad (\text{V.3})$$

where $\epsilon_{0,B}^2 := \frac{n_x}{\sigma_{p,0}^2} \log \frac{1}{\delta}$ and $c_5 := c_2 \left\| C \right\| \left\| \text{Cond}(\Phi_{p,0}\Phi_{p,0}) \right\|$.

Third, the cross-term error can be rewritten as

$$\begin{aligned} \tilde{C}^E &= \Sigma_e^{1/2}E_{f1}Z_p^\top \hat{L}_p^\top (\hat{L}_p Z_p Z_p^\top \hat{L}_p^\top)^{-1} \\ &= \Sigma_e^{1/2}E_{f1}Z_p^\top (Z_p Z_p^\top)^{-1} \text{Cond}(\Phi_{p,0}\Phi_{p,0}). \end{aligned}$$

Similar to bounding $\tilde{\Theta}_i^E$ in Lemma 2, by taking $i = 0$, \tilde{C}^E is bounded by

$$\left\| \tilde{C}^E \right\| \leq \frac{c_6 \epsilon_{0,E}^2}{N}, \quad (\text{V.4})$$

where $c_6 := c_1 \left\| \text{Cond}(\Phi_{p,0}\Phi_{p,0}) \right\|$, and $\epsilon_{0,E}$ is given by taking $i = 0$ in $\epsilon_{i,E}$ in (35). After merging (V.2), (V.3) and (V.4) together, we obtain (45a).

2) *Bounds on A and B*: We first rewrite (23b) as

$$\begin{aligned}\hat{X}_k^+ &= T^\top \bar{A} \hat{X}_k + T^\top \bar{B} U_{f1} + K \Sigma_e^{1/2} E_{f1} + \\ &\quad T^\top \bar{A} T (T^\top \bar{X}_k - \hat{X}_k) + (\hat{X}_k^+ - T^\top \bar{X}_k^+).\end{aligned}$$

According to (25b), the estimates of A and B is

$$\hat{\theta} := [\hat{A} \quad \hat{B}] = \hat{X}_k^+ \begin{bmatrix} \hat{X}_k \\ U_{f1} \end{bmatrix}^\dagger. \quad (\text{V.5})$$

For brevity, we define

$$\bar{\theta} := [T^\top \bar{A} T \quad T^\top \bar{B}], \quad \Psi_k := \begin{bmatrix} \hat{X}_k \\ U_{f1} \end{bmatrix} = \hat{L}_{p,1} \Phi_{p,1},$$

where $\hat{L}_{p,1} = \begin{bmatrix} \hat{L}_p & 0 \\ 0 & I \end{bmatrix}$, and $\Phi_{p,1} = \begin{bmatrix} Z_p \\ U_{f1} \end{bmatrix}$. In this way, the estimation error of θ can be similarly divided into three parts:

$$\tilde{\theta} := \hat{\theta} - \bar{\theta} = \tilde{\theta}^L + \tilde{\theta}^B + \tilde{\theta}^E,$$

where

$$\begin{aligned}\tilde{\theta}^L &:= T^\top \bar{A} T (\hat{L}_p - T^\top \bar{L}_p) Z_p \Psi_k^\dagger + (\hat{L}_p - T^\top \bar{L}_p) Z_p^+ \Psi_k^\dagger, \\ \tilde{\theta}^B &:= A A_K^p X_{k-p} \Psi_k^\dagger + A_K^p X_{k-p}^+ \Psi_k^\dagger, \\ \tilde{\theta}^E &:= K \Sigma_e^{1/2} E_{f1} \Psi_k^\dagger.\end{aligned}$$

First, for $\tilde{\theta}^L$, we rewrite it as

$$\begin{aligned}\tilde{\theta}^L &:= T^\top \bar{A} T (\hat{L}_p - T^\top \bar{L}_p) Z_p \Phi_{p,1}^\top \hat{L}_{p,1}^\top \left(\hat{L}_{p,1} \Phi_{p,1} \Phi_{p,1}^\top \hat{L}_{p,1}^\top \right)^{-1} \\ &\quad + (\hat{L}_p - T^\top \bar{L}_p) Z_p^+ \Phi_{p,1}^\top \hat{L}_{p,1}^\top \left(\hat{L}_{p,1} \Phi_{p,1} \Phi_{p,1}^\top \hat{L}_{p,1}^\top \right)^{-1}.\end{aligned}$$

For convenience, we define

$$\text{Cond}(\Phi_{p,1} \Phi_{p,1}^\top) = \hat{L}_{p,1} \Phi_{p,1} \Phi_{p,1}^\top \hat{L}_{p,1}^\top \left(\hat{L}_{p,1} \Phi_{p,1} \Phi_{p,1}^\top \hat{L}_{p,1}^\top \right)^{-1}.$$

Similar to $\text{Cond}(\Phi_{p,0} \Phi_{p,0}^\top)$, we conclude that $\text{Cond}(\Phi_{p,1} \Phi_{p,1}^\top)$ grows at most logarithmically with N . Then, we have that

$$\|\tilde{\theta}^L\| \leq c_7 \|\hat{L}_p - T^\top \bar{L}_p\|, \quad (\text{V.6})$$

where $c_7 := (\|T^\top \bar{A} T\| + \|I\|) \|\text{Cond}(\Phi_{p,1} \Phi_{p,1}^\top)\|$.

Second, for $\tilde{\theta}^B$, we rewrite it as

$$\begin{aligned}\tilde{\theta}^B &:= A A_K^p X_{k-p} \Phi_{p,1}^\top \hat{L}_{p,1}^\top \left(\hat{L}_{p,1} \Phi_{p,1} \Phi_{p,1}^\top \hat{L}_{p,1}^\top \right)^{-1} + \\ &\quad A_K^p X_{k-p}^+ \Phi_{p,1}^\top \hat{L}_{p,1}^\top \left(\hat{L}_{p,1} \Phi_{p,1} \Phi_{p,1}^\top \hat{L}_{p,1}^\top \right)^{-1},\end{aligned}$$

which can be bounded by

$$\|\tilde{\theta}^B\| \leq c_8 \frac{\epsilon_{1,B}}{N}, \quad (\text{V.7})$$

where $c_8 = \|A + I\| \|\text{Cond}(\Phi_{p,1} \Phi_{p,1}^\top)\|$, and $\epsilon_{1,B}$ is in (37).

Third, for $\|\tilde{\theta}^E\|$, we rewrite it as

$$\tilde{\theta}^E := K \Sigma_e^{1/2} E_{f1} \Phi_{p,1}^\top \hat{L}_{p,1}^\top \left(\hat{L}_{p,1} \Phi_{p,1} \Phi_{p,1}^\top \hat{L}_{p,1}^\top \right)^{-1},$$

which can be bounded by

$$\|\tilde{\theta}^E\| \leq c_9 \frac{\epsilon_{1,E}}{\sqrt{N}}, \quad (\text{V.8})$$

where $c_9 = \|K \Sigma_e^{1/2}\| \|\text{Cond}(\Phi_{p,1} \Phi_{p,1}^\top)\|$, and $\epsilon_{1,E}$ is in (35). After merging (V.6), (V.7) and (V.8) together, we obtain (45b). We hence complete the proof. \blacksquare

B. Proof of Theorem 5.3 (MOESP Type Realization)

The proof of Theorem 5.3 is identical to [32, Th. 4], thus, it is omitted here. \blacksquare

APPENDIX VI TECHNICAL LEMMAS

Lemma 8 ([52, Lemma 6]): Norm of a sub-Gaussian vector: For an entry-wise σ_w^2 -sub-Gaussian random variable $w \in \mathbb{R}^{n_w}$, i.e., such that $\log \mathbb{E} [e^{\lambda w}] \leq \mathbb{E} [w] \lambda + \frac{\sigma_w^2 \lambda^2}{2}$ for all $\lambda \in \mathbb{R}$, with probability at least $1 - \delta/2$, for $1 \leq k \leq N$,

$$\|w\| \leq \sigma_w n_w \sqrt{2n_w \log(32Nn_w/\delta)}.$$

Lemma 9: Let M_1, \dots, M_N be random matrices in $\mathbb{R}^{n \times n}$. Let $W \in \mathbb{R}^{n \times n}$ be a fixed symmetric matrix. Let $S_N = \sum_{i=1}^N M_i$ and $\tilde{S}_N = \sum_{i=1}^N \tilde{M}_i$, where $\tilde{M}_i = M_i \mathbb{1}_{\{M_i \preceq W\}}$ is the truncated version of M_i . Then it holds that

$$\mathbb{P}(S_N \succ V) \leq \mathbb{P}\left(\max_{1 \leq i \leq N} M_i \succ W\right) + \mathbb{P}(\tilde{S}_N \succ V).$$

Proof: The proof closely follows the proof of the scalar case [52, Lemma 14], thus, it is omitted here. \blacksquare

Lemma 10 ([53, Th. 7.1]): Matrix Azuma: Consider a finite adapted sequence $\{W_k\}$ of self-adjoint matrices of dimension d , and a fixed sequence $\{M_k\}$ of self-adjoint matrices that satisfy $\mathbb{E}_{k-1} W_k = 0$ and $M_k^2 \succcurlyeq W_k^2$ almost surely. Then, for all $t \geq 0$, $\mathbb{P}\{\lambda_{\max}(\sum_k W_k) \geq t\} \leq d \cdot \exp\left(-\frac{t^2}{8\|\sum_k M_k^2\|}\right)$.

Lemma 11 ([54]): Weyl's inequality: Let $M_1, M_2 \in \mathbb{R}^{n \times n}$ be Hermitian matrices, with eigenvalues ordered in descending order $\lambda_1 \geq \lambda_2 \geq \dots \geq \lambda_n$. Then, for $i + j > n$,

$$\lambda_{i+j-1}(M_1 + M_2) \leq \lambda_i(M_1) + \lambda_j(M_2) \leq \lambda_{i+j-n}(M_1 + M_2).$$

Lemma 12 ([55, Th. 12]): Markov's inequality: Let a matrix $M \succ 0$, and a random matrix $W \succcurlyeq 0$ almost surely. Then, we have $\mathbb{P}(W \not\preceq M) \leq \text{trace}(\mathbb{E} W M^{-1})$, where $(W \not\preceq M)$ is the complement of the event $(W \preceq M)$.

Lemma 13 ([56, Th. 3.4]): Self-normalized martingale: Let $\{\mathcal{F}_k\}_{k=0}^N$ be a filtration such that $\{W_k\}_{k=1}^N$ is adapted to $\{\mathcal{F}_{k-1}\}_{k=1}^N$ and $\{V_k\}_{k=1}^N$ is adapted to $\{\mathcal{F}_k\}_{k=1}^N$. Additionally, suppose that for all $1 \leq k \leq N$, $V_k \in \mathbb{R}^{n_v \times 1}$ is σ^2 -conditionally sub-Gaussian with respect to \mathcal{F}_k . Let $\Sigma \in \mathbb{R}^{n_w \times n_w}$. Given a failure probability $0 < \delta < 1$, then with probability at least $1 - \delta$, we have

$$\begin{aligned}\left\| \sum_{k=1}^N V_k W_k^\top \left(\Sigma + \sum_{k=1}^N W_k W_k^\top \right)^{-1/2} \right\|^2 &\leq 8n_v \sigma^2 \log 5 + \\ 4\sigma^2 \log \left(\frac{\det(\Sigma + \sum_{k=1}^N W_k W_k^\top)}{\det(\Sigma)} \right) + 8\sigma^2 \log \frac{1}{\delta}.\end{aligned}$$

Lemma 14 ([57], [42, Th. 2.1]): Hanson-Wright inequality: Consider a random variable $w \in \mathbb{R}^{n_w}$, where each entry is a scalar, zero mean and independent σ_w^2 -sub-Gaussian random variable. For a matrix $M \in \mathbb{R}^{n_w \times n_w}$ and every $s \geq 0$, we have

$$\begin{aligned}\mathbb{P}(\|w^\top M w - \mathbb{E} w^\top M w\| > s) &\leq \\ 2\exp\left(-\min\left(\frac{s^2}{114\sigma_w^4 \|M\|_F^2}, \frac{s}{16\sqrt{2}\sigma_w^2 \|M\|}\right)\right).\end{aligned}$$

Lemma 15 (Lemma A.1 in [32]): Norm of a block matrix: Let a block matrix $M = [M_1^\top \quad M_2^\top \quad \dots \quad M_f^\top]^\top$, where

all the sub-matrices M_i 's have the same dimension. Then, the block matrix M satisfies $\|M\| \leq \sqrt{f} \max_{1 \leq i \leq f} \|M_i\|$.

Lemma 16: Shur complement: Let $M = \begin{bmatrix} M_1 & M_2 \\ M_2^\top & M_4 \end{bmatrix}$ be a block matrix, and $M_4 \succ 0$. Defining $M_S = M_1 - M_2 M_4^{-1} M_2^\top$ as the Shur complement of M , we then have

$$1) M^{-1} = \begin{bmatrix} M_S^{-1} & -M_S^{-1} M_2 M_4^{-1} \\ -M_4^{-1} M_2^\top M_S^{-1} & M_\Delta \end{bmatrix}, \text{ where } M_\Delta = M_4^{-1} + M_4^{-1} M_2^\top M_S^{-1} M_2 M_4^{-1}.$$

2) $M \succ 0$, if and only if $M_S \succ 0$.

3) If $M \succ 0$, then $\lambda_{\max}(M) \geq \lambda_{\max}(M_S)$.

4) If $M \succ 0$, then $\lambda_{\min}(M) \leq \lambda_{\min}(M_S)$.

Proof: Given that $M_4 \succ 0$, then M can be rewritten as

$$M = \begin{bmatrix} I & M_2 M_4^{-1} \\ 0 & I \end{bmatrix} \begin{bmatrix} M_S & 0 \\ 0 & M_4 \end{bmatrix} \begin{bmatrix} I & 0 \\ M_4^{-1} M_2^\top & I \end{bmatrix}.$$

The first and second statements can then be obtained straightforwardly. For the third statement, since $M_S \prec M_1$, we have $\lambda_{\max}(M_S) \leq \lambda_{\max}(M_1) \leq \lambda_{\max}(M)$. For the forth statement, according to the first statement, since $\lambda_{\max}(M^{-1}) \geq \lambda_{\max}(M_S^{-1})$, so $\lambda_{\min}(M) \leq \lambda_{\min}(M_S)$. \blacksquare

Lemma 17 ([32, Th. 4]): Suppose rank n matrices M and \bar{M} have singular value decomposition $U\Lambda V^\top$ and $\bar{U}\bar{\Lambda}\bar{V}^\top$, where \bar{M} is the rank n approximation of \hat{M} . If $\|M - \hat{M}\| \leq \frac{\sigma_n(M)}{4}$, then there exists a unitary matrix T such that

$$\max \left(\left\| \bar{U}\bar{\Lambda}^{1/2} - U\Lambda^{1/2}T \right\|, \left\| \bar{\Lambda}^{1/2}\bar{V}^\top - T^\top\Lambda^{1/2}V^\top \right\| \right) \leq \kappa_M,$$

$$\text{where } \kappa_M = \sqrt{\frac{40n}{\sigma_n(M)}} \|M - \hat{M}\|.$$

Lemma 18 ([58, Th. 4.1]): Consider matrices $M_1, M_2 \in \mathbb{R}^{m \times n}$ with rank m , where $m \leq n$. Then, we have

$$\|M_1^\dagger - M_2^\dagger\| \leq \sqrt{2} \|M_1^\dagger\| \|M_2^\dagger\| \|M_1 - M_2\|.$$

Lemma 19 ([32, Lemma E.2]): Consider the series $W_t = \sum_{k=0}^t \|A^k\|$. We have the following two cases:

- 1) If the system is asymptotically stable, i.e., $\rho(A) < 1$, then $\|W_t\| = \mathcal{O}(1)$.
- 2) If the system is marginally stable, i.e., $\rho(A) = 1$, then $\|W_t\| = \mathcal{O}(t^\kappa)$, where κ is the Largest Jordan block of A corresponding to the eigenvalue $|\lambda| = 1$.

Lemma 20 ([32, Lemma B.5]): Let $\beta \geq b > 0$, for some $b > 0$ and consider the function:

$$f(\alpha, \beta) = \frac{\alpha + \beta}{2} - \gamma\sqrt{\alpha + 1},$$

for $a \geq 0$. If $\gamma \leq \min(1, \frac{b}{2})$, then $f(\alpha, \gamma) \geq 0$.